Ann. Inst. H. Poincaré D
Comb. Phys. Interact. 9 (2022), 159–218
DOI 10.4171/AIHPD/117

Notes on tensor models and tensor field theories

Razvan Gurau

Abstract. Tensor models and tensor field theories admit a $1/N$ expansion and a melonic large N limit which is simpler than the planar limit of random matrices and richer than the large N limit of vector models. They provide examples of analytically tractable but non-trivial strongly coupled quantum field theories and lead to a new class of conformal field theories. We present a compact introduction to the topic, covering both some of the classical results in the field, like the details of the $1/N$ expansion, as well as recent developments. These notes are loosely bases on four lectures given at the Journées de physique mathématique Lyon 2019: Random tensors and SYK models.

Contents

1. Introduction

Quantum field theory (QFT) [109] accurately describes both the fundamental interactions in nature (like the electroweak [40, 95, 104] and strong [37] interactions) and condensed matter systems (like Ising spins [63] or Fermi liquids [81]). In particular, it gives one of the most precise predictions in physics: the electron anomalous magnetic moment up to 10^{-10} relative error. Perhaps the most important lesson of

2020 Mathematics Subject Classification. 81T32.
Keywords. Tensor field theory.

quantum field theory is that physics changes with the energy scale, as captured by the renormalization group [88, 105, 106].

By and large QFT has two regimes. On the one hand, one has weakly coupled theories, like quantum electrodynamics. As the name suggests, these theories are almost free and the effect of interactions is well accounted for in perturbation theory. Making sense rigorously of the perturbative expansion is quite non-trivial [41]. However, given the right circumstances, perturbative computations yield very accurate predictions. On the other hand, one has strongly coupled theories, which are famously difficult to deal with. While successful numerical approaches have been developed, like lattice quantum chromodynamics, analytical results are much harder to come by. Two prominent strategies exist to deal with strongly coupled QFTs analytically.

One strategy is to consider theories endowed with constraining symmetries or integrability properties. For instance, at a fixed point of the renormalization group a QFT becomes scale invariant and, more often than not, scale invariant theories are in fact conformally invariant. Conformal invariance is a very strong constraint [28] which allows one to bootstrap a plethora of results [98].

A second strategy consists in identifying new parameters, not related to the strength of the interaction, and attempt a perturbative study with respect to them. An example of this is the so called "large N" field theory [82]. If the quantum field itself is a vector (or a matrix or a tensor) in some Hilbert space of dimension N, one can attempt to study the theory in a $1/N$ expansion. This is a three step strategy.

- Take N large (infinite). In this limit the theory simplifies. The $1/N$ expansion is useful as long as the large N limit is rich enough to be non-trivial, but simple enough to be more manageable than the original theory.
- Compute the corrections to the large N behavior order by order in $1/N$, at all orders.
- Resum the $1/N$ series or bound the rest.

This strategy brings mixed results. With the exception of some models in dimension zero[1] [53, 58, 73], step 3 is almost never considered. Step 2 is again considered mostly in dimension zero [14, 17, 26, 30, 42, 61, 62, 93]. Beyond the fact that the second and third step are seldom manageable, the two classical examples of a vector [12, 100] or a matrix [101] field are somewhat disappointing already at step 1. Vector models

[1] By dimension we mean the dimension of the space or space-time on which the vector, matrix or tensor field theory is defined, that is QCD is a theory in 4 dimensions [101]. In matrix and tensor models [27, 55] there is a second notion of dimension: the Feynman diagrams have non-trivial topology and encode combinatorial triangulations in various dimensions (two in the case of QCD). Thus [27] deals with matrix models in 0 dimensions, although they are relevant for two-dimensional quantum gravity.

are analytically tractable in the large N limit and have plenty of applications [11,82].[2] However, they are limited by the fact that at leading order in $1/N$ vector models do not give an anomalous scaling dimension for the field. Consequently, one is stuck with either numerical studies [49] or almost classical scaling. On the contrary, matrix models [16,27,101] are too complicated to be resummed in the large N (planar) limit, in more than zero dimension.

Tensor models [55, 70] give a new class of large N field theories. They exhibit a *melonic* large N limit [13, 55] which is different from both the vector and the matrix ones. Vector-tensor models and some regimes of matrix models also lead to a melonic limit [3, 4, 31, 32]. Unsurprisingly, the melonic limit is richer than the large N limit of vectors. Surprisingly, although as algebraic objects tensors are more complicated than matrices, the melonic limit is simpler than the planar one.

Tensor models have been extensively studied in zero dimensions (where they were originally introduced and studied as models of quantum gravity [2, 10, 50, 60, 85, 96, 97]) and in one dimension (e.g., [19, 21, 23, 56, 65, 67, 68, 72, 77, 78, 83, 86, 108]) because they provide an alternative to the Sachdev–Ye–Kitaev model [33, 43, 45, 46, 66, 80, 89, 94] without quenched disorder. Some small N tensor models can also be solved analytically [67,75,76,83]. Higher-dimensional tensor field theories have been more recently explored [6, 7, 38, 39, 90, 91]. At large N and in the infrared these theories typically yield conformal field theories (CFTs) of a new kind which we call by extension melonic.

Melonic theories are an ideal compromise between solvability and richness: contrary to almost all the other examples of strongly interacting theories, they can be treated analytically. To a large extent, they can be studied disregarding their origin. This is reflected in the organization of these notes. In Section 2 we present a brief overview of conformal field theories and the particular features of the melonic ones. In Section 3 we present several models which become melonic in the large N limit. Section 4 presents an effective action formalism well adapted to tensor field theories and finally Section 5 presents in detail the renormalization group flow, fixed points and infrared melonic CFT in one model. The appendices collect some technical details.

Notation. We work in Euclidean $\mathbb{R}^d$. We sometimes denote integrals over positions by $\int_x \equiv \int d^d x$ and integrals over momenta by $\int_p \equiv \int \frac{d^d p}{(2\pi)^d}$. The Fourier transform is $f(p) = \int_x e^{\mathrm{i}\, px} f(x)$ with inverse $f(x) = \int_p e^{-\mathrm{i}\, px} f(p)$. Repeated indices are summed.

[2] They provide for instance explicit CFT duals to Fradkin–Vasiliev higher spin theories [34, 35, 69, 102].

2. Melonic field theories

Melonic conformal field theories are a new class of analytically accessible CFTs. We first briefly review CFT in d dimensions and then explain what makes melonic theories special. The reader can find plenty of references on conformal field theories. Here we present a brief digest of [79, 99]. We use the notation in [79].[3]

2.1. A digest of conformal field theories

In Euclidean $\mathbb{R}^d$ with line element $dx^2 = \delta_{\mu\nu}\, dx^\mu\, dx^\nu$ conformal transformations $x \to x'(x)$ preserve the line element up to a local scale factor $dx'^2 = \Omega(x)^2 dx^2$. The infinitesimal[4] conformal transformations $x'^\mu = x^\mu + v^\mu$, $\Omega = 1 + \sigma$ are generated by

$$v_\mu(x) = a_\mu + \omega_{\mu\nu}x^\nu + \kappa x_\mu + b_\mu x^2 - 2x_\mu b\cdot x, \quad \omega_{\mu\nu} = -\omega_{\nu\mu}, \quad \sigma = \kappa - 2b\cdot x. \tag{2.1}$$

The conformal group has $\binom{d+2}{2}$ generators and is locally isomorphic to $\mathrm{SO}(d+1,1)$. A general conformal transformation is such that

$$\frac{\partial x'^\mu}{\partial x^\nu} = \Omega(x) R^\mu_\nu(x), \quad \delta_{\mu\nu} R^\mu_\sigma(x) R^\nu_\rho(x) = \delta_{\sigma\rho}, \quad \Omega(x) = \left|\frac{\partial x'^\mu}{\partial x^\nu}\right|^{\frac{1}{d}}, \tag{2.2}$$

and

$$(x'_1 - x'_2)^2 = \Omega(x_1)\Omega(x_2)(x_1 - x_2)^2.$$

Conformally invariant cross ratios can be built starting with four positions

$$(x^2_{ij}x^2_{kl})/(x^2_{ik}x^2_{jl}),$$

where $x_{ij} = x_i - x_j$.

The irreducible representations of $\mathrm{SO}(d)$ are classified by the spin. For bosonic fields, the representation space of the spin J representation consists in symmetric traceless tensors with J indices. We denote multi-indices by

$$\bar{\mu} = \mu_1 \dots \mu_J.$$

[3] This section is the author's synopsis of the four lectures given by V. Rosenhaus at the Journées de physique mathématique Lyon 2019: Random tensors and SYK models. The author would like to take this opportunity to thank him for many clarifying discussions on the topic.

[4] The finite transformations are translations $x'^\mu = x^\mu + a^\mu$, rotations $x'^\mu = R^\mu_\nu x^\nu$, dilatations $x'^\mu = \Lambda x^\mu$ and special conformal transformations $x'^\mu = (x^\mu + x^2 b^\mu)/(1 + 2b\cdot x + b^2x^2)$.

The rotation R^{μ}_{ν} is represented in the representation J by the tensor product

$$R^{\bar{\mu}}_{\bar{\nu}} = R^{\mu_1}_{\nu_1} \dots R^{\mu_J}_{\nu_J}.$$

In a scalar theory, for instance, a spin J composite operator is

$$[(\partial^2)^{n_1} \partial_{(\mu_1} \dots \partial_{\mu_i} \phi][\partial_{\mu_{i+1}} \dots \partial_{\mu_J)} (\partial^2)^{n_2} \phi] - \text{traces}.$$

The primary operators $O_{\Delta,J}$ in a conformal field theory (CFT) are vectors in the spin representation J and change under the conformal transformation in (2.2) as[5]

$$O'^{\bar{\mu}}_{\Delta,J}(x') = \Omega(x)^{-\Delta} R^{\bar{\mu}}_{\bar{\nu}}(x) O^{\bar{\nu}}_{\Delta,J}(x), \tag{2.3}$$

where Δ and J are the scaling dimension and the spin of the operator and $R^{\bar{\mu}}_{\bar{\nu}}(x)$ is the matrix representing the rotation $R^{\mu}_{\nu}(x)$ in the spin representation J.

The two and three point functions of primary operators are fixed by conformal invariance [29, 99]. The two point function is non-zero only for operators of the same dimension and spin:

$$\langle O^{\bar{\mu}}_{\Delta,J}(x_1) O_{\Delta,J;\bar{\nu}}(x_2)\rangle = \frac{I^{\mu_1}_{(\nu_1}(x_{12}) \dots I^{\mu_J}_{\nu_J)}(x_{12}) - \text{traces}}{|x_{12}|^{2\Delta}}, \quad I^{\mu}_{\nu}(x) = \delta^{\mu}_{\nu} - 2\frac{x^{\mu} x_{\nu}}{|x|^2}; \tag{2.4}$$

while the three point function of two spin zero operators ϕ_1 and ϕ_2 with dimensions Δ_1 and Δ_2 and a spin J operator $O_{\Delta,J}$ is

$$\begin{aligned} &\langle \phi_1(x_1)\phi_2(x_2) O_{\Delta,J;\bar{\mu}}(x_3)\rangle \\ &\quad = C^{\Delta_1,\Delta_2}_{\Delta,J} \frac{Z_{\mu_1} \dots Z_{\mu_J} - \text{traces}}{|x_{12}|^{\Delta_1+\Delta_2-\Delta+J} |x_{13}|^{\Delta+\Delta_1-\Delta_2-J} |x_{23}|^{\Delta+\Delta_2-\Delta_1-J}}, \end{aligned} \tag{2.5a}$$

$$Z_{\mu} = \Big(\frac{(x_{13})_{\mu}}{|x_{13}|^2} - \frac{(x_{23})_{\mu}}{|x_{23}|^2}\Big), \tag{2.5b}$$

where $C^{\Delta_1,\Delta_2}_{\Delta,J}$ are pure numbers.

The operator product expansion (OPE) in quantum field theory expresses the product of two operators at nearby points as a sum of local operators. For a scalar field theory this is written schematically as

$$\phi(x_1)\phi(x_2) \simeq \sum C(x_{12}^2) x_{12}^{\mu_1} \dots x_{12}^{\mu_J} O_{\mu_1 \dots \mu_J}(x_2) \quad \text{for } x_1 \sim x_2.$$

[5] In components, the infinitesimal transformation of primary fields is

$$\delta O^{\bar{\alpha}}_{\Delta,J} = -v^{\mu} \partial_{\mu} O^{\bar{\alpha}}_{\Delta,J} - (\kappa - 2b \cdot x) \Delta O^{\bar{\alpha}}_{\Delta,J} + \frac{1}{2}[\omega^{\mu\nu} - 2(b^{\mu} x^{\nu} - b^{\nu} x^{\mu})](s_{\mu\nu})^{\bar{\alpha}}_{\bar{\beta}} O^{\bar{\beta}}_{\Delta,J},$$

where $s_{\mu\nu}$ denotes the spin matrices in the representation J. The spin matrices are the generators of the $so(d)$ Lie algebra $[s_{\mu\nu}, s_{\rho\sigma}] = \delta_{\mu\rho} s_{\nu\sigma} - \delta_{\nu\rho} s_{\mu\sigma} - \delta_{\mu\sigma} s_{\nu\rho} + \delta_{\nu\sigma} s_{\mu\rho}$. In the vector representation for instance we have $(s_{\mu\nu})_{ab} = \delta_{\mu b}\delta_{\nu a} - \delta_{\nu b}\delta_{\mu a}$.

This equality should be interpreted in the weak sense, that is it is valid when inserted in arbitrary correlations. In a conformal field theory the OPE is strongly constrained by conformal invariance[6] and the sum restricts to primary operators [29, 84]:

$$\phi_1(x_1)\phi_2(x_2) = \sum_{\Delta,J} C_{\Delta,J}^{\Delta_1,\Delta_2} P_{\Delta,J}^{\Delta_1,\Delta_2;\bar{\mu}}(x_{12},\partial_{x_2}) O_{\Delta,J;\bar{\mu}}(x_2), \tag{2.6}$$

with the OPE coefficients $C_{\Delta,J}^{\Delta_1,\Delta_2}$ given by (2.5) and $P_{\Delta,J}^{\Delta_1,\Delta_2;\bar{\mu}}(x_{12},\partial_{x_2})$ some universal differential operator fixed by conformal invariance which captures the contribution of the primary $O_{\Delta,J}$ and all its descendants. For instance, the three point function of three spin zero operators is at the same time given by (2.5) and by the OPE, hence

$$\frac{1}{|x_{12}|^{\Delta_1+\Delta_2-\Delta}|x_{13}|^{\Delta_1+\Delta-\Delta_2}|x_{23}|^{\Delta_2+\Delta-\Delta_1}} = P_{\Delta}^{\Delta_1,\Delta_2}(x_{12},\partial_{x_2})\frac{1}{|x_{23}|^{2\Delta}}, \tag{2.7}$$

where we omitted the spin index. The polynomial $P_{\Delta}^{\Delta_1,\Delta_2}(x_{12},\partial_{x_2})$ is obtained by substituting $x_{13} = x_{12} + x_{23}$ in the left-hand side and Taylor expanding[7] in x_{12}.

Arbitrary correlation functions in a conformal field theory can be computed by applying the OPE iteratively, therefore a CFT is completely specified by the list of primary operators and OPE coefficients. We will now present a method for computing the dimensions of (some of) the physical primary operators and (some of) the OPE coefficients in a CFT.

Our starting point is a four point function. To simplify our life, we consider correlations with four spin zero fields. Applying the OPE twice in the channel (12)(34) yields

$$\langle\phi_1(x_1)\phi_2(x_2)\phi_3(x_3)\phi_4(x_4)\rangle = \sum_{\Delta,J} C_{\Delta,J}^{\Delta_1,\Delta_2} C_{\Delta,J}^{\Delta_3,\Delta_4} G_{\Delta,J}^{\Delta_i}(x_i), \tag{2.8}$$

where the universal functions $G_{\Delta,J}^{\Delta_i}(x_i)$, the conformal blocks [25], are known explicitly. The four point function can be re expressed in terms of conformal partial waves [79, 99] as we now explain.

For any primary operator $O_{\Delta,J}$, we define its shadow $\widetilde{O}_{\widetilde{\Delta},J}$ to be an operator with the same spin but with dimension $\widetilde{\Delta} = d - \Delta$. Let us denote by $\langle\dots\rangle^{\text{cs}}$ the conformal structure of a correlation function, given by (2.4) and (2.5) with the OPE

[6] As an example, note that any operator in a CFT, primary or not, will change under global dilatations by a rescaling $O'(\Lambda x) = \Lambda^{-\Delta_O} O(x)$ which fixes $C(x_{12}^2) \sim |x_{12}|^{-2\Delta_\phi+\Delta_O-J}$.

[7] At first orders we get

$$P_{\Delta}^{\Delta_1,\Delta_2}(x_{12},\partial_{x_2}) = |x_{12}|^{\Delta-\Delta_1-\Delta_2}\Big(1 + \frac{\Delta+\Delta_1-\Delta_2}{2\Delta} x_{12}^{\mu}\partial_{x_2^{\mu}} + \cdots\Big).$$

coefficients set to 1. The shadow coefficient [79] of three operators $S_{O_1}^{O_2O_3}$ is defined by the equation

$$\int d^d y \langle \widetilde{O}_{\widetilde{\Delta},J;\bar{\nu}}(x_1)\widetilde{O}^{\bar{\mu}}_{\widetilde{\Delta},J}(y)\rangle^{\mathrm{cs}}\langle O_{\Delta,J;\bar{\mu}}(y)O_2(x_2)O_3(x_3)\rangle^{\mathrm{cs}}$$
$$= S_O^{O_2O_3}\langle \widetilde{O}_{\widetilde{\Delta},J;\bar{\nu}}(x_1)O_2(x_2)O_3(x_3)\rangle^{\mathrm{cs}}, \tag{2.9}$$

where from now on we assume we deal with real fields (otherwise the spin representation should be conjugated). We have for instance [79]

$$S_{\Delta,J}^{\Delta_1,\Delta_2} = \pi^{\frac{d}{2}}\frac{\Gamma\left(\Delta-\frac{d}{2}\right)\Gamma(\Delta+J-1)\Gamma\left(\frac{\widetilde{\Delta}+\Delta_1-\Delta_2+J}{2}\right)\Gamma\left(\frac{\widetilde{\Delta}-\Delta_1+\Delta_2+J}{2}\right)}{\Gamma(\Delta-1)\Gamma(d-\Delta+J)\Gamma\left(\frac{\Delta+\Delta_1-\Delta_2+J}{2}\right)\Gamma\left(\frac{\Delta-\Delta_1+\Delta_2+J}{2}\right)}, \tag{2.10a}$$

$$S_{\Delta_2}^{\Delta_1,(\Delta,J)} = \pi^{\frac{d}{2}}\frac{\Gamma\left(\Delta_2-\frac{d}{2}\right)\Gamma\left(\frac{\widetilde{\Delta}_2+\Delta_1-\Delta+J}{2}\right)\Gamma\left(\frac{\widetilde{\Delta}_2+\Delta-\Delta_1+J}{2}\right)}{\Gamma(d-\Delta_2)\Gamma\left(\frac{\Delta_2+\Delta_1-\Delta+J}{2}\right)\Gamma\left(\frac{\Delta_2+\Delta-\Delta_1+J}{2}\right)}. \tag{2.10b}$$

Let us define the conformal partial waves:

$$\Psi_{\Delta,J}^{\Delta_i} = \int dx_0 \langle \phi_1(x_1)\phi_2(x_2)O^{\bar{\mu}}_{\Delta,J}(x_0)\rangle^{\mathrm{cs}}\langle \widetilde{O}_{\widetilde{\Delta},J;\bar{\mu}}(x_0)\phi_3(x_3)\phi_4(x_4)\rangle^{\mathrm{cs}}. \tag{2.11}$$

Using the conformal scaling in the first three point conformal structure, one can show after some effort [99] that the conformal partial wave is a sum of the conformal block $G_{\Delta,J}^{\Delta_i}(x_i)$ and its shadow block $G_{\widetilde{\Delta},J}^{\Delta_i}(x_i)$:

$$\Psi_{\Delta,J}^{\Delta_i} = \left(-\frac{1}{2}\right)^J S_{\widetilde{\Delta},J}^{\Delta_3,\Delta_4}G_{\Delta,J}^{\Delta_i}(x_i) + \left(-\frac{1}{2}\right)^J S_{\Delta,J}^{\Delta_1,\Delta_2}G_{\widetilde{\Delta},J}^{\Delta_i}(x_i). \tag{2.12}$$

A complete set of partial waves $\Psi_{\Delta,J}^{\Delta_i}$ is obtained in $d>1$ by choosing integer spin J and the dimensions $\Delta = d/2 + \mathrm{i}\, r, r \geq 0$ (for $d=1$ one needs to add the discrete set $\Delta = 2n, n \geq 1$). These dimensions do not correspond to physical primary operators. The functions are orthogonal [99]:

$$(\Psi_{\Delta,J}^{\Delta_i}, \Psi_{\widetilde{\Delta}',J'}^{\widetilde{\Delta}_i}) = \int \frac{\prod_{i=1}^4 d^d x_i}{\mathrm{Vol}(\mathrm{SO}(d+1,1))}\Psi_{\Delta,J}^{\Delta_i}(x_i)\Psi_{\widetilde{\Delta}',J'}^{\widetilde{\Delta}_i}(x_i)$$
$$= 2\pi n_{\Delta,J}\delta(r-r')\delta_{JJ'}, \tag{2.13a}$$

$$n_{\Delta,J} = \frac{S_{\widetilde{\Delta},J}^{\Delta_3,\Delta_4}S_{\Delta,J}^{\widetilde{\Delta}_3,\widetilde{\Delta}_4}\,\mathrm{Vol}(S^{d-2})}{\mathrm{Vol}(\mathrm{SO}(d-1))}$$
$$\times \frac{\pi(2J+d-2)\Gamma(J+1)\Gamma(J+d-2)}{2^{2J+d-2}\Gamma\left(J+\frac{d}{2}\right)^2}, \tag{2.13b}$$

with $\Delta = d/2 + \mathrm{i}\, r$, $\widetilde{\Delta}' = d/2 - \mathrm{i}\, r'$ and $r, r' > 0$.

Now, let us consider a field theory (not necessarily conformal) for a scalar field ϕ, such that the one point function is zero. The four point function is a sum of a disconnected contribution (12)(34) and the part connecting (12) and (34):

$$\langle\phi(x_1)\phi(x_2)\phi(x_3)\phi(x_4)\rangle = \langle\phi(x_1)\phi(x_2)\rangle\langle\phi(x_3)\phi(x_4)\rangle + \langle\phi(x_1)\phi(x_2)\phi(x_3)\phi(x_4)\rangle_{12\to 34}. \tag{2.14}$$

The correlation $\langle\dots\rangle_{12\to 34}$ can be written in term of the irreducible four point kernel (see Section 4 for details). Expressing the self-energy Σ (that is the one particle irreducible two point function) in terms of the dressed two point function G, the irreducible four point kernel is the functional derivative of Σ with respect to G:

$$K(x_1, x_2; x_3, x_4) = \int d^d x_a d^d x_b G(x_{1a}) G(x_{2b}) \frac{\delta\Sigma(x_{34})}{\delta G(x_{ab})}, \tag{2.15}$$

and the four point function connecting (12) and (34) is

$$\langle\phi(x_1)\phi(x_2)\phi(x_3)\phi(x_4)\rangle_{12\to 34} = \int d^d x_a d^d x_b \Big(\frac{1}{1-K}\Big)(x_1, x_2; x_a x_b)\big(G(x_{a3})G(x_{b4}) + (a \leftrightarrow b)\big). \tag{2.16}$$

In a CFT in which the field ϕ is a primary operator with dimension Δ_ϕ, as the partial waves form a basis, equation (2.14) becomes

$$\langle\phi(x_1)\phi(x_2)\phi(x_3)\phi(x_4)\rangle = \frac{1}{|x_{12}|^{2\Delta_\phi}} \frac{1}{|x_{34}|^{2\Delta_\phi}} + \sum_J \int_{\frac{d}{2}}^{\frac{d}{2}+\mathrm{i}\infty} \frac{d\Delta}{2\pi\,\mathrm{i}} \rho(\Delta, J) \Psi^{\Delta_\phi}_{\Delta,J}(x_i), \tag{2.17}$$

where the field is normalized so that the two point function is exactly the conformal structure. The disconnected term is the contribution to the OPE of the identity operator with dimension and spin 0. All the other physical operators and the OPE coefficients are captured by the density $\rho(\Delta, J)$. This density can be computed by expanding (2.16) on partial waves. We first expand the rightmost term in (2.16):

$$\begin{aligned}\langle\phi(x_1)\phi(x_3)\rangle\langle\phi(x_2)\phi(x_4)\rangle + (1 \leftrightarrow 2) &= \mathcal{F}^0(x_i) \\ &= \sum_J \int_{\frac{d}{2}}^{\frac{d}{2}+\mathrm{i}\infty} \frac{d\Delta}{2\pi\,\mathrm{i}} \rho^0(\Delta, J) \Psi^{\Delta_\phi}_{\Delta,J}(x_i),\end{aligned} \tag{2.18}$$

where $\rho^0(\Delta, J) = (\mathcal{F}^0, \Psi^{\tilde{\Delta}_\phi}_{\tilde{\Delta},J})/n_{\Delta,J}$. The first term in the scalar product is, substituting the partial wave (and denoting arguments as indices),

$$\int \frac{d^d x_i d^d x_0}{\mathrm{Vol}(\mathrm{SO}(d+1,1))} \langle \phi_{x_1}\phi_{x_3}\rangle \langle \phi_{x_2}\phi_{x_4}\rangle \langle \tilde{\phi}_{x_1}\tilde{\phi}_{x_2}\widetilde{O}^{\bar{\mu}}_{\tilde{\Delta},J}(x_0)\rangle^{\mathrm{cs}} \langle O_{\Delta,J;\bar{\mu}}(x_0)\tilde{\phi}_{x_3}\tilde{\phi}_{x_4}\rangle^{\mathrm{cs}}$$
$$= S^{\tilde{\Delta}_\phi,(\Delta,J)}_{\tilde{\Delta}_\phi} S^{\Delta_\phi,(\Delta,J)}_{\tilde{\Delta}_\phi} \int \frac{dx_1 dx_2 dx_0}{\mathrm{Vol}(\mathrm{SO}(d+1,1))} \langle \tilde{\phi}_{x_1}\tilde{\phi}_{x_2}\widetilde{O}^{\bar{\mu}}_{\tilde{\Delta},J}(x_0)\rangle^{\mathrm{cs}}$$
$$\times \langle O_{\Delta,J;\bar{\mu}}(x_0)\phi_{x_1}\phi_{x_2}\rangle^{\mathrm{cs}}, \quad (2.19)$$

where we computed the integrals over x_3 and x_4 using (2.9). The remaining integral is just a pure number [79] which we denote by t_0:

$$t_0 = \frac{1}{\mathrm{Vol}(\mathrm{SO}(d-1))} \frac{\Gamma\left(\frac{d-2}{2}\right)\Gamma(J+d-2)}{2^J \Gamma(d-2)\Gamma\left(J+\frac{d-2}{2}\right)}. \quad (2.20)$$

Taking into account the symmetry properties of the conformal three point function, we get

$$\rho^0(\Delta, J) = \frac{1+(-1)^J}{n_{\Delta,J}} t_0 S^{\tilde{\Delta}_\phi,(\Delta,J)}_{\tilde{\Delta}_\phi} S^{\Delta_\phi,(\Delta,J)}_{\tilde{\Delta}_\phi}. \quad (2.21)$$

Now, due to conformal invariance, the irreducible four point kernel applied on a three point function must be proportional to the three point function:

$$\int dx_3^d dx_4^d K(x_1, x_2; x_3, x_4)\langle \phi(x_3)\phi(x_4) O^{\bar{\mu}}_{\Delta,J}(x)\rangle$$
$$= k(\Delta, J)\langle \phi(x_1)\phi(x_2) O^{\bar{\mu}}_{\Delta,J}(x)\rangle; \quad (2.22)$$

therefore

$$\rho(\Delta, J) = \frac{1}{1-k(\Delta, J)} \rho^0(\Delta, J). \quad (2.23)$$

Putting everything together, inserting the partial wave in terms of the conformal blocks and noting that $\rho(\tilde{\Delta}, J) = \rho(\Delta, J)$ we get

$$\langle \phi(x_1)\phi(x_2)\phi(x_3)\phi(x_4)\rangle_{12\to 34}$$
$$= \sum_J \int_{\frac{d}{2}-\mathrm{i}\infty}^{\frac{d}{2}+\mathrm{i}\infty} \frac{d\Delta}{2\pi\,\mathrm{i}} \frac{1}{1-k(\Delta, J)} \frac{1+(-1)^J}{n_{\Delta,J}} t_0$$
$$\times S^{\tilde{\Delta}_\phi,(\Delta,J)}_{\tilde{\Delta}_\phi} S^{\Delta_\phi,(\Delta,J)}_{\tilde{\Delta}_\phi} \left(-\frac{1}{2}\right)^J S^{\Delta_\phi\Delta_\phi}_{\tilde{\Delta},J} G^{\Delta_\phi}_{\Delta,J}(x_i). \quad (2.24)$$

In order to find the OPE coefficients and the dimension of the primaries, we close the integral contour on the right half complex plane. The integral then becomes a sum over the poles of the integrand. There are many poles: some come from the conformal

block itself, some from the explicit S factors and some from the $(1-k(\Delta,J))^{-1}$ factor. It turns out that some of the poles are spurious [99], and only the poles of $1/(1-k(\Delta,J))$ are physical. We denote by Δ_n the solutions of the equation $k(\Delta,J)=1$. These are the dimensions of the physical primary operators present in the OPE of $\phi\phi$ in (2.6), and

$$\langle\phi(x_1)\phi(x_2)\phi(x_3)\phi(x_4)\rangle_{12\to34} = \sum_J \sum_n (C^{\Delta_\phi\Delta_\phi}_{\Delta_n,J})^2 G^{\Delta_\phi}_{\Delta_n,J}(x_i), \tag{2.25a}$$

$$(C^{\Delta_\phi\Delta_\phi}_{\Delta_n,J})^2 = -\operatorname{Res}\Big(\frac{1}{1-k(\Delta,J)};\Delta_n\Big)\frac{1+(-1)^J}{n_{\Delta_n,J}}t_0 \times S^{\tilde\Delta_\phi,(\Delta_n,J)}_{\tilde\Delta_\phi} S^{\Delta_\phi,(\Delta_n,J)}_{\tilde\Delta_\phi}\Big(-\frac{1}{2}\Big)^J S^{\Delta_\phi\Delta_\phi}_{\tilde\Delta_n,J}. \tag{2.25b}$$

This method for computing the dimensions of the physical primary operators and the OPE coefficients is completely general. However, it is of limited use in the most generic case because the four point kernel and consequently $k(\Delta,J)$ are complicated.

2.2. The melonic truncation

We now introduce a class of field theories which we call *melonic*. In these theories one is able to close the equation (2.25) and compute $k(\Delta,J)$ analytically.

Let us consider the simple example of a scalar field theory with a q-body interaction ϕ^q in zero dimensions. The "field" ϕ is just a real variable and the action and partition function write

$$S = \frac{1}{2}\phi C^{-1}\phi + \frac{\lambda}{q!}\phi^q, \quad \mathcal{Z} = \int [d\phi] e^{-S}, \tag{2.26}$$

where $C>0$ is the covariance (propagator) and λ the coupling. Of course in this case one can eliminate the covariance C by a rescaling, but we refrain from doing this.

The partition function and correlations can be evaluated by Taylor expanding in the coupling and computing the Gaussian integrals.[8] This leads to the standard Feynman graph representation. The graphs have vertices with coordination q and, for correlation functions, external points with coordination 1. The connected two point function of the model

$$G = \langle\phi\phi\rangle_c = \frac{1}{\mathcal{Z}}\int [d\phi] e^{-S}\phi\phi - \Big(\frac{1}{\mathcal{Z}}\int [d\phi] e^{-S}\phi\Big)^2, \tag{2.27}$$

[8] For ϕ_A a vector in some vector space and C_{AB} some non-negative operator, the moments of the normalized Gaussian measure of covariance C are computed by the Wick theorem:

$$\int [d\phi] e^{-\frac{1}{2}\phi_A C^{-1}_{AB}\phi_B}\phi_{A_1}\dots\phi_{A_{2p}} = \sum_{\text{pairings }\Pi}\prod_{\{i,j\}\in\Pi} C_{A_iA_j}, \quad [d\phi] \equiv (\det C)^{-1/2}\prod_A d\phi_A.$$

is a sum over connect graphs with two external points. It obeys the Schwinger–Dyson equation (SDE) depicted in Figure 1:

$$G^{-1} = C^{-1} - \Sigma, \tag{2.28}$$

where the *self energy* Σ is the sum of amputated, one particle irreducible (1PI) two point graphs.

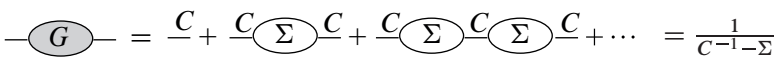

Figure 1. The Schwinger–Dyson equation.

The SDE can be closed by re expressing the self energy back in terms of the two point function G. Usually this is not very useful as the self energy is a complicated sum over two particle irreducible graphs (more details on this in Section 4).

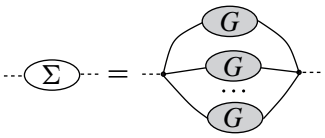

Figure 2. The melonic truncation of the self energy.

The melonic truncation is a truncation of the self energy which leads to a non-trivial but manageable SDE. It consists in restricting the self energy to the *melon* graph depicted in Figure 2 which is made of two vertices connected by $q-1$ parallel two point functions.[9] In zero dimensions the melonic truncation reads

$$\Sigma = \Big[\frac{\lambda^2}{(q-1)!}\Big] G^{q-1}. \tag{2.29}$$

We put the combinatorial factor in square brackets as it is the only thing which depends on the details of the model. We call a theory melonic if this truncation holds.

In a zero-dimensional melonic theory, combining (2.28) and (2.29) one can solve for the two point function

$$\begin{aligned} G &= C + C\Big[\frac{\lambda^2}{(q-1)!}\Big] G^q \\ \Longrightarrow\ G &= \sum_{n\geq 0} \frac{1}{qn+1}\binom{qn+1}{n}\Big(\Big[\frac{\lambda^2}{(q-1)!}\Big] C^q\Big)^n C. \end{aligned} \tag{2.30}$$

[9] The melonic truncation of the self energy defines melonic two point graphs. Vacuum melonic graphs are obtained by reconnecting the external edges of a (not necessarily one particle irreducible) two point graph into an edge.

Now, let us go to higher dimensions. The SDE in a melonic theory in d dimensions is

$$(G^{-1})(x_1,x_2) = (C^{-1})(x_1,x_2) - \Sigma(x_1,x_2), \quad \Sigma(x) = \Big[\frac{\lambda^2}{(q-1)!}\Big][G(x)]^{q-1}, \tag{2.31}$$

where G^{-1} (and C^{-1}) denotes the operator inverse and we used translation invariance in the second equation. We now attempt to solve for the two point function self consistently. This is possible if one ignores the free covariance. Taking a conformal ansatz for the two point function,

$$G(x_1-x_2) = b\frac{1}{|x_1-x_2|^{2\Delta_\phi}}, \tag{2.32}$$

and going to momentum space[10] the SDE in a melonic theory is solved by

$$\Delta_\phi = \frac{d}{q}, \quad \Big[\frac{\lambda^2}{(q-1)!}\Big]b^q = \frac{\Gamma(\Delta_\phi)\Gamma(d-\Delta_\phi)}{\pi^d(-1)\Gamma\big(\frac{d}{2}-\Delta_\phi\big)\Gamma\big(-\frac{d}{2}+\Delta_\phi\big)}. \tag{2.33}$$

The attentive reader will note that this solution is only formal: the presence of an Euler Γ function with a negative argument stems form the fact that the Fourier transform of the right-hand side of (2.31) is in fact divergent. We will be treating this equation rigorously in Section 5. Observe that the melonic truncation already expresses the self energy in terms of the two point function. The irreducible four point kernel is then readily obtained:

$$\begin{aligned} K(x_1,x_2;x_3,x_4) &= \int d^dx_a d^dx_b G(x_{1a})G(x_{2b})\frac{\delta\Sigma(x_{34})}{\delta G(x_{ab})} \\ &= (q-1)\Big[\frac{\lambda^2}{(q-1)!}\Big]G(x_{13})G(x_{24})G(x_{34})^{q-2}. \end{aligned} \tag{2.34}$$

In order to close (2.25), we need to determine $k(\Delta, J)$. The trick is to note that, as $\Delta_\phi = d/q$, we have

$$\frac{1}{|x_{34}|^{\Delta_\phi(q-2)}}\langle\phi(x_3)\phi(x_4)O^{\bar\mu}_{\Delta,J}(x_0)\rangle^{\rm cs} = \langle\tilde\phi(x_3)\tilde\phi(x_4)O^{\bar\mu}_{\Delta,J}(x_0)\rangle^{\rm cs}; \tag{2.35}$$

[10] Recall the Fourier transform:

$$\int_x \frac{e^{ipx}}{x^{2a}} = \frac{\pi^{d/2}\Gamma\big(\frac{d}{2}-a\big)}{2^{2a-d}\Gamma(a)}\frac{1}{p^{d-2a}}.$$

therefore

$$\int dx_3 dx_4 K(x_1, x_2; x_3 x_4) \langle \phi(x_3)\phi(x_4) O^{\bar{\mu}}_{\Delta,J}(x_0)\rangle^{\text{cs}}$$
$$= (q-1)\Big[\frac{\lambda^2}{(q-1)!}\Big] b^q$$
$$\times \int dx_3 dx_4 \langle \phi(x_1)\phi(x_3)\rangle^{\text{cs}} \langle \phi(x_2)\phi(x_4)\rangle^{\text{cs}} \langle \tilde{\phi}(x_3)\tilde{\phi}(x_4) O^{\bar{\mu}}_{\Delta,J}(x_0)\rangle^{\text{cs}}. \tag{2.36}$$

The integrals can now be computed using the shadow coefficients in (2.9) and we get

$$k(\Delta, J) = (q-1)\Big[\frac{\lambda^2}{(q-1)!}\Big] b^q S^{\tilde{\Delta}_\phi,(\Delta,J)}_{\tilde{\Delta}_\phi} S^{\Delta_\phi,(\Delta,J)}_{\tilde{\Delta}_\phi}, \tag{2.37}$$

which, with the help of (2.10), yields

$$k(\Delta, J) = (q-1)\frac{\beth}{\Re}, \tag{2.38}$$

where

$$\beth = \Gamma(d-\Delta_\phi)\Gamma\Big(\frac{d}{2}-\Delta_\phi\Big)\Gamma\Big(\Delta_\phi - \frac{d}{2} + \frac{\Delta+J}{2}\Big)\Gamma\Big(\Delta_\phi - \frac{\Delta-J}{2}\Big),$$
$$\Re = (-1)\Gamma\Big(-\frac{d}{2}+\Delta_\phi\Big)\Gamma(\Delta_\phi)\Gamma\Big(d-\Delta_\phi-\frac{\Delta-J}{2}\Big)\Gamma\Big(\frac{d}{2}-\Delta_\phi+\frac{\Delta+J}{2}\Big).$$

3. The melonic limit as a large N limit

Melonic theories lead to analytically controlled CFTs in the infrared limit. However, in the previous section the melonic truncation appeared as a trick designed to produce a solvable model.

The important question then becomes: is there any natural way to obtain a melonic limit in a field theory? The answer to this question is yes: in the case of tensor field theories the melonic limit is naturally obtained at large N. In fact, when a random tensor is present, the large N limit will often be melonic. In particular, as we will see below, models mixing vectors and tensors also fall in this class.

In this section we present three models which exhibit a melonic large N limit. We only deal for now with the combinatorial aspects of this limit and, in order to simplify the discussion, we will present the models in dimension zero. We will go back to field theories in the next section.

The models we discuss here deal with non-symmetric tensors. It should be mentioned that there exist models for symmetric tensors (in rank 3) for which the large N limit has been proven to be melonic [5, 20, 21, 57, 71]. However, the proofs are significantly more involved for model with symmetries.

3.1. The colored tensor model

This model is sometimes called the Gurau–Witten model [50, 60, 108]. It can be formulated for arbitrary rank tensors. For all the ranks it has a large N limit dominated by melonic graphs [13]. The classification of graphs at any order in $1/N$ has been performed [56, 61].

Let us consider $D+1$ tensor fields of rank D. We denote the fields by $T^i_{A^i}$, where $i = 0, \ldots, D$ is the *color* of T^i and the multi index A^i is $A^i = \{a^i_j \mid j \neq i\}$. All the indices a go from 1 to N and the tensors have no symmetry property. For example in rank $D = 3$ the list of fields is

$$T^0_{a^0_1 a^0_2 a^0_3} \equiv T^0_{A^0}, \quad T^1_{a^1_0 a^1_2 a^1_3} \equiv T^1_{A^1}, \quad T^2_{a^2_0 a^2_1 a^2_2} \equiv T^2_{A^2}, \quad T^3_{a^3_0 a^3_1 a^3_2} \equiv T^3_{A^3}. \tag{3.1}$$

Observe that the indices a have two colors. We set $\delta_{A^i B^i} = \prod_{j\neq i} \delta_{a^i_j b^i_j}$.

The model has a global symmetry group $\mathcal{O}(N)^{D(D+1)/2}$ consisting in an orthogonal transformation $O^{(ij)} = O^{(ji)} \in \mathcal{O}(N)$ for each couple of colors (ij). Under the action of the symmetry group, *both* indices a^i_j and a^j_i transform in the fundamental representation of $O^{(ij)}$. In detail, the global symmetry acts on T^i as

$$(T')^i_{B^i} = \prod_{j\neq i} O^{(ij)}_{b^i_j a^i_j} T^i_{A^i}, \quad B^i = \{b^i_j | j \neq i\}, \quad A^i = \{a^i_j | j \neq i\}. \tag{3.2}$$

For example, in rank 3 we have $O^{(10)} = O^{(01)}$ and so on and the fields transform as

$$(T')^0_{b^0_1 b^0_2 b^0_3} = O^{(01)}_{b^0_1 a^0_1} O^{(02)}_{b^0_2 a^0_2} O^{(03)}_{b^0_3 a^0_3} T_{a^0_1 a^0_2 a^0_3}, \tag{3.3a}$$

$$(T')^1_{b^1_0 b^1_2 b^1_3} = O^{(10)}_{b^1_0 a^1_0} O^{(12)}_{b^1_2 a^1_2} O^{(13)}_{b^1_3 a^1_3} T_{a^1_0 a^1_2 a^1_3}, \tag{3.3b}$$

etc. The action and partition function of the model are

$$S = \frac{1}{2}\sum_i T^i_{A^i} C^{-1} T^i_{A^i} + \frac{\lambda}{N^{D(D-1)/4}} \prod_{i<j} \delta_{a^i_j a^j_i} \prod_i T^i_{A^i}, \quad \mathcal{Z} = \int [dT] e^{-S}, \tag{3.4}$$

where we have included a redundant covariance C for the Gaussian part. Due to the global symmetry the two point functions of the model are diagonal both in the colors and in the indices:

$$\langle T^i_{A^i} T^j_{B^j} \rangle_c = \delta^{ij} \delta_{A^i B^i} G, \quad G = C + C\lambda\partial_\lambda (N^{-D} \ln \mathcal{Z}). \tag{3.5}$$

G is obtained by taking a two point function, contracting its external indices respecting the colors and dividing by N^D.

The partition function and the correlations can be computed in the Feynman expansion. The Feynman graphs are $D+1$-valent and the edges have a color $i =$

$0, \ldots, D$. One can give a detailed, *stranded*, representation of the Feynman graphs adapted to tracking the indices of the tensor. This is represented in Figure 3 for $D = 3$. Each tensor is represented as a half edge with D strands, one for each one of its indices. $D + 1$ half edges meet at a vertex and for every couple of half edges two strands (representing the indices a^i_j and a^j_i) are joined. The edges transmit D strands.

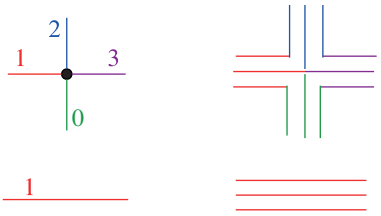

Figure 3. The vertex and the propagator of the colored tensor model in rank $D = 3$.

The vacuum Feynman graphs are edge $(D + 1)$-colored graphs [50, 60]. A graph $\mathcal{G}$ has

- $V(\mathcal{G})$ vertices of coordination $D + 1$;
- $\frac{D+1}{2}V(\mathcal{G})$ edges colored $0, 1 \ldots, D$ such that at every vertex we have exactly one edge of each color;
- $F(\mathcal{G})$ *faces*, that is bicolored cycles.

The faces track the indices of the tensors: the indices are transmitted along the edges and turn around vertices, thus an index $a^i_j = a^j_i$ follows the face (ij) and we get a free sum (hence a factor N) whenever the face closes. Open graphs arising in the Feynman expansion of correlations have additional external points corresponding to the external field insertions and open strands connecting pairs of external indices.

In order to compute G in (3.5), we use a trick (depicted in Figure 4): we contract the external indices of a two point function respecting the colors and divide by N^D. We denote by $\mathfrak{G}$ the set of rooted,[11] connected edge $(D + 1)$-colored graphs and we get

$$\begin{aligned} G &= \frac{1}{N^D}\delta_{A^i B^i}\langle T^i_{A^i} T^i_{B^i}\rangle_c \\ &= \sum_{\mathcal{G}\in\mathfrak{G}} (-\lambda)^{V(\mathcal{G})} C^{\frac{D+1}{2}V(\mathcal{G})+1} N^{-D-\frac{D(D-1)}{4}V(\mathcal{G})+F(\mathcal{G})}, \end{aligned} \tag{3.6}$$

[11] A rooted graph is a graph with one edge (the root) marked by an arrow. For colored graphs we fix the color of the root edge.

where the root edge represents the external contraction $\delta_{A^i B^i}$. Remarkably, every rooted graph with unlabeled vertices has a combinatorial factor 1. Observe that $\mathfrak{G}$ contains a graph with no vertices (on the left in Figure 4). It corresponds to the Gaussian pairing of the two external tensors and brings a covariance C.

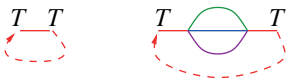

Figure 4. Rooted graphs.

The crucial fact is that the numbers of faces and vertices of a connected graph $\mathcal{G}$ are related [51, 52, 59] by the following relation (see Proposition 3 and Appendix A):

$$F(\mathcal{G}) = D + \frac{D(D-1)}{4} V(\mathcal{G}) - \hat{\omega}(\mathcal{G}), \quad \hat{\omega}(\mathcal{G}) \geq 0, \tag{3.7}$$

where the *reduced degree* $\hat{\omega}(\mathcal{G})$ of a graph $\mathcal{G}$ is a non-negative half-integer. The properties of the degree are discussed in detail in Appendix A. The two point function (and all the other correlation functions) admits a $1/N$ expansion indexed by the degree:

$$G = \sum_{\hat{\omega} \in \mathbb{N}/2} N^{-\hat{\omega}} \sum_{\mathcal{G} \in \mathfrak{G}}^{\hat{\omega}(\mathcal{G}) = \hat{\omega}} (-\lambda)^{V(\mathcal{G})} C^{\frac{D+1}{2} V(\mathcal{G}) + 1}. \tag{3.8}$$

At leading order one obtains only the graphs with $\hat{\omega}(\mathcal{G}) = 0$. The graphs of degree zero are the melonic graphs [13], see Proposition 4, Appendix A. Opening a rooted melonic vacuum graph at the root one obtains a melonic two point graph and at leading order:

$$(G^{\mathrm{LO}})^{-1} = C^{-1} - \Sigma^{\mathrm{LO}}, \quad \Sigma^{\mathrm{LO}} = \lambda^2 (G^{\mathrm{LO}})^D. \tag{3.9}$$

3.2. The colored tensor–vector model

This model is the zero-dimensional counterpart of the Sachdev–Ye–Kitaev model [43, 54, 66, 80, 89, 94]. It comes in two flavors, quenched and annealed, which coincide at the first few orders. Although more involved, the sub leading corrections have been classified also in this case [36].

The model consists in D vectors $\psi^i_{a_i}$ (distinguished by the color i) coupled by a random coupling $T_{a_1,\dots,a_D}$. The random coupling is a rank-D tensor with no symmetries distributed on a Gaussian. The action of the model is

$$S = \frac{1}{2} \sum_i \psi^i_{a_i} C^{-1} \psi^i_{a_i} + \lambda T_{a_1 \dots a_D} \prod_i \psi^i_{a_i}. \tag{3.10}$$

We set

$$T \cdot T \equiv T_{a_1 \dots a_D} T_{a_1 \dots a_D}$$

and

$$[dT] = \prod_{a_1 \dots a_D} N^{(D-1)/2} dT_{a_1 \dots a_D}.$$

One can either take the quenched or the annealed averages over the random couplings. Consequently, one has the quenched and the annealed free energies, the quenched and the annealed two point functions, and so on. Denoting $\mathcal{Z}(T) = \int [d\psi] \exp\{-S\}$ we have

$$\mathcal{F}^{(q)} = \frac{1}{N} \int [dT] e^{-\frac{N^{D-1}}{2} T \cdot T} \ln(\mathcal{Z}(T)), \tag{3.11a}$$

$$\mathcal{F}^{(a)} = \frac{1}{N} \ln\left(\int [dT] e^{-\frac{N^{D-1}}{2} T \cdot T} \mathcal{Z}(T) \right), \tag{3.11b}$$

$$\langle \psi^i_{a_i} \psi^j_{a_j} \rangle^{(q)}_c = \int [dT] e^{-\frac{N^{D-1}}{2} T \cdot T} \frac{1}{\mathcal{Z}(T)} \int [d\psi] e^{-S} \psi^i_{a_i} \psi^j_{a_j}, \tag{3.11c}$$

$$\langle \psi^i_{a_i} \psi^j_{a_j} \rangle^{(a)}_c = \frac{1}{\int [dT] e^{-\frac{N^{D-1}}{2} T \cdot T} \mathcal{Z}(T)} \int [dT] e^{-\frac{N^{D-1}}{2} T \cdot T} \int [d\psi] e^{-S} \psi^i_{a_i} \psi^j_{a_j}, \tag{3.11d}$$

The two point functions (both the quenched and the annealed one) are again diagonal in the colors and in the indices:

$$\langle \psi^i_{a_i} \psi^j_{a_j} \rangle^{(q),(a)}_c = \delta^{ij} \delta_{a_i a_j} G^{(q),(a)}. \tag{3.12}$$

The Feynman graphs are still edge $(D+1)$-colored graphs: 0 is the color of the tensor (disorder) averages and $1, \dots, D$ are the colors of the vector contractions. One can give a stranded represent in which the tensor has D strands and the vectors only one strand as depicted in Figure 5 on the right.

Figure 5. Colored and stranded representation of the vertex of the tensor–vector model in rank $D = 3$.

From the point of view of the index contractions, the edge 0 is very different from the others: the edges $1,\dots,D$ carry an index each, while the edge 0 carries D indices. By the same trick as before, the two point functions can be expressed as sums over rooted (the root has color $i \neq 0$) connected edge $(D+1)$-colored graphs:

$$\begin{aligned} G^{(q),(a)} &= \frac{1}{N}\delta_{a_i a_j}\langle \psi^i_{a_i}\psi^j_{a_j}\rangle^{(q),(a)}_c \\ &= \sum_{\mathcal{G}\in\mathfrak{G}^{(q),(a)}} (-\lambda)^{V(\mathcal{G})} C^{\frac{D}{2}V(\mathcal{G})+1} N^{-1-(D-1)V(\mathcal{G})+\sum_i F^{(0i)}(\mathcal{G})}, \end{aligned} \tag{3.13}$$

where $F^{(0i)}$ denotes the number of faces with colors $(0i)$ of $\mathcal{G}$.

Contrary to the colored tensor model, we now get a free sum (hence a factor N) only for the faces involving the color 0: it is quite clear in the stranded representation of Figure 5 that there is no index going from the edge 1 to the edge 2. Therefore, the faces (12), which are the bicolored cycles made by edges of colors 1 and 2 do not contribute to the amplitude. It is convenient to add and subtract the missing faces, (ij) with $i, j \neq 0$. The number of faces which involve the color zero is the total number of faces minus the number of faces which do not involve the color 0:

$$\sum_i F^{(0i)}(\mathcal{G}) = \sum_{0\leq i<j\leq D} F^{(ij)}(\mathcal{G}) - \sum_{1\leq i<j\leq D} F^{(ij)}(\mathcal{G}). \tag{3.14}$$

The only difference between the quenched and annealed models is the class of graphs over which we sum. In the annealed case we sum over all the (rooted) connected edge $(D+1)$-colored graphs $\mathfrak{G}^{(a)} \equiv \mathfrak{G}$. For the quenched case, we sum only over the (rooted) connected edge $(D+1)$-colored graphs which remain connected after deleting all the edges of color 0. We denote the set of graphs with this property by $\mathfrak{G}^{(q)}$.

Let $\mathcal{G}$ be a connected edge $(D+1)$-colored graph, and let us denote by $\mathcal{G}^0$ the edge D-colored graph obtained from $\mathcal{G}$ by deleting the edges of color 0 (which correspond to the disorder averages). In general, $\mathcal{G}^0$ can be disconnected and we denote by $C(\mathcal{G}^0) \geq 1$ the number of connected components of $\mathcal{G}^0$. As $\mathcal{G}^0$ is an edge D-colored graph, it has a reduced degree $\hat{\omega}(\mathcal{G}^0)$ and the total number of its faces is given by (3.7) with D shifted to $D-1$. We define the SYK degree of $\mathcal{G}$ to be $\hat{\Omega}(\mathcal{G}) = \hat{\omega}(\mathcal{G}) - \hat{\omega}(\mathcal{G}^0)$. This number is a half-integer which obeys the bounds (see Proposition 5 in Appendix A)

$$\frac{1}{D}\hat{\omega}(\mathcal{G}) \leq \Omega(\mathcal{G}) \leq \hat{\omega}(\mathcal{G}), \tag{3.15}$$

hence, in particular, it is non-negative. A straightforward computation yields

$$G^{(q),(a)} = \sum_{\mathcal{G}\in\mathfrak{G}^{(q),(a)}} (-\lambda)^{V(\mathcal{G})} C^{\frac{D}{2}V(\mathcal{G})+1} N^{-\left[C(\mathcal{G}^0)-1\right](D-1)-\Omega(\mathcal{G})}. \tag{3.16}$$

For the quenched model, we always have $C(\mathcal{G}^0) = 1$, but, for the annealed model, $C(\mathcal{G}^0) \geq 1$. However, in the large N limit, both the quenched and the annealed models are dominated by graphs with $C(\mathcal{G}^0) = 1$ and $\Omega(\mathcal{G}) = 0$. The quenched and the annealed models coincide up to the order $N^{-(D-1)}$. If one uses the replica trick to compute the quenched averages, the departure between the quenched and the annealed models signals a replica symmetry breaking.

The SYK degree $\Omega(\mathcal{G})$ is non-negative and is zero for a connected graph $\mathcal{G}$ if and only if $\mathcal{G}$ is melonic. If $\mathcal{G}$ is melonic, then $\mathcal{G}^0$ is a union of melonic graphs. At leading order $\mathcal{G}^0$ is furthermore connected, hence it consists in exactly one melonic graph.[12] Therefore, at leading order we get

$$(G^{\mathrm{LO}})^{-1} = C^{-1} - \Sigma^{\mathrm{LO}}, \quad \Sigma^{\mathrm{LO}} = \lambda^2 (G^{\mathrm{LO}})^{D-1}. \tag{3.17}$$

The annealed model (and consequently the quenched model at first orders) can be simplified by introducing "bilocal" fields integrating over the disorder:

$$\begin{aligned}
&\int [dT][d\psi] e^{-S} \\
&\quad = \int [d\psi] e^{-\frac{1}{2}\sum_i \psi^i_{a_i} C^{-1} \psi^i_{a_i} + \frac{\lambda^2}{2N^{D-1}} \prod_i \psi^i_{a_i} \psi^i_{a_i}} \\
&\qquad \times \int [dG^i][d\Sigma^i] e^{-\frac{1}{2}\sum_i \Sigma^i (NG^i - \psi^i_{a_i} \psi^i_{a_i})} \\
&\quad = \int [dG^i][d\Sigma^i][d\psi] e^{-\frac{1}{2}\sum_i \psi_{a_i} (C^{-1} - \Sigma^i) \psi_{a_i} - N(\frac{1}{2}\sum_i G^i \Sigma^i - \frac{\lambda^2}{2} \prod_i G^i)} \\
&\quad = \int [dG^i][d\Sigma^i] e^{-N(\pm\frac{1}{2}\sum_i \mathrm{Tr}\ln(1 - C\Sigma^i) + \frac{1}{2}\sum_i G^i \Sigma^i - \frac{\lambda^2}{2}\prod_i G^i)},
\end{aligned} \tag{3.18}$$

where the $-$ sign is obtained for fermionic vectors (which requires even rank D), the $+$ sign for bosonic ones, and we took into account that the Gaussian integral over the vector fields is normalized. The advantage of this representation is that N is an overall scaling and the $1/N$ expansion is a standard saddle point approximation. The saddle point equations write (using the fact that the saddle is color symmetric)

$$\Sigma - \lambda^2 G^{D-1} = 0, \quad G - \frac{1}{C^{-1} - \Sigma} = 0, \tag{3.19}$$

which reproduce the SDE in the melonic limit (3.17). The $1/N$ expansion is obtained by computing the saddle point corrections. However, we stress that this gives the $1/N$ expansion of the annealed model, hence fails to reproduce the one of the quenched case starting with the order $N^{-(D-1)}$.

[12] Observe that in this case one can uniquely reconstruct $\mathcal{G}$ starting from $\mathcal{G}^0$.

3.3. The $\mathcal{O}(N)^3$ model

This model is sometimes called *Carrozza–Tanasa–Klebanov–Tarnopolsky model* [22, 39, 72]. As the name suggests, the model is defined only for rank-3 tensors. Its interest resides in the fact that it includes all the radiative corrections for quartic interactions, hence a field theory built on it is well adapted to a renormalization group study. At leading order the model is dominated by a *melon-tadpole* graphs, a slight generalization of melons. The first sub leading orders of this model are understood [8, 22].

The field of the model is a rank-3 non-symmetric tensor $\phi_A = \phi_{a_1 a_2 a_3}$ transforming in the three fundamental representation of $\mathcal{O}(N) \otimes \mathcal{O}(N) \otimes \mathcal{O}(N)$, that is under a change of basis each index turns with its own orthogonal transformation

$$(\phi')_{b_1 b_2 b_3} = O^{(1)}_{b_1 a_1} O^{(2)}_{b_2 a_2} O^{(3)}_{b_3 a_3} \phi_{a_1 a_2 a_3}. \tag{3.20}$$

One can consider the slightly more general case of a $\mathcal{O}(N_1) \otimes \mathcal{O}(N_2) \otimes \mathcal{O}(N_3)$ symmetry, but we will refrain from doing this here. We denote by capital letters triples of indices: $A = \{a_1, a_2, a_3\}$ and so on and we define three patters of contraction of indices among four tensors:

$$\delta^t_{ABCD} = (\delta_{a_1 b_1} \delta_{c_1 d_1})(\delta_{a_2 c_2} \delta_{b_2 d_2})(\delta_{a_3 d_3} \delta_{b_3 c_3}), \tag{3.21a}$$

$$\delta^p_{AB;CD} = \frac{1}{3} \sum_j \delta_{a_j c_j} \delta_{b_j d_j} \Big(\prod_{i \neq j} \delta_{a_i b_i} \delta_{c_i d_i} \Big), \quad \delta^d_{AB;CD} = \prod_i \delta_{a_i b_i} \delta_{c_i d_i}. \tag{3.21b}$$

The first pattern δ^t_{ABCD} is called the *tetrahedral* pattern, the second one $\delta^p_{AB;CD}$ the *pillow* and the third one the *double trace*. The action of the model is

$$S = \frac{1}{2} \phi_A C^{-1} \phi_A + \Big(\frac{\lambda}{4N^{3/2}} \delta^t_{ABCD} + \frac{\lambda_p}{4N^2} \delta^p_{AB;CD} + \frac{\lambda_d}{4N^3} \Big) \phi_A \phi_B \phi_C \phi_D, \tag{3.22}$$

and the two point function is diagonal in the tensor indices $\langle \phi_A \phi_B \rangle = \delta_{AB} G$.

Again, one can compute the partition function and correlations in a Feynman expansion. The Feynman graphs of the CTKT model are stranded graph made of stranded vertices connected by stranded edges, as depicted in Figure 6. The strands are associated to the indices of the tensors. All the vertices are four valent and the edges have three strands. The strands have a color and close into the faces of the graph. The faces correspond, again, to free sums over indices. From left to right in Figure 6, we represented the tetrahedral, the pillow and the double trace vertex. There are three kinds of pillow vertices, as a function of the special color which is transmitted from on pair of half edges to the other.

We denote by $V_t(\mathcal{G})$, $V_p(\mathcal{G})$, and $V_d(\mathcal{G})$ the numbers of tetrahedral, pillow and double trace vertices of a CTKT graph $\mathcal{G}$, and $F(\mathcal{G})$ the number of faces of $\mathcal{G}$. The number of pillow vertices splits as the sum of the numbers of pillow vertices of each

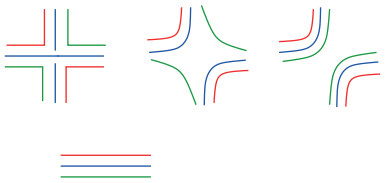

Figure 6. Vertices and edges of the CTKT model.

kind. The edges are not colored, but the faces are colored with a color 1, 2, or 3. Using the same trick as before, we can compute the two point function by reconnecting the external edges and dividing by N^3, obtaining G as a sum over rooted graphs:

$$G = \sum_{\mathcal{G}\in\mathfrak{G}} (-\lambda)^{V_t(\mathcal{G})}\Big(-\frac{\lambda_p}{3}\Big)^{V_p(\mathcal{G})}(-\lambda_d)^{V_d(\mathcal{G})} \times C^{2[V_t(\mathcal{G})+V_p(\mathcal{G})+V_d(\mathcal{G})]+1} N^{-3-\frac{3}{2}V_t(\mathcal{G})-2V_p(\mathcal{G})-3V_d(\mathcal{G})+F(\mathcal{G})}. \quad (3.23)$$

As in the case of the colored model, the number of faces of a CTKT graph can be computed in terms of the number of vertices (see Proposition 6 in Appendix A):

$$F(\mathcal{G}) = 3 + \frac{3}{2}V_t(\mathcal{G}) + 2V_p(\mathcal{G}) + 3V_d(\mathcal{G}) - \omega(\mathcal{G}), \quad (3.24)$$

where the CTKT degree $\omega(\mathcal{G})$ is a non-negative half-integer. The two point function (and any other correlation) has a $1/N$ expansion indexed by the CTKT degree:

$$G = \sum_{\omega\in\mathbb{N}/2} N^{-\omega} \sum_{\mathcal{G}\in\mathfrak{G}}^{\omega(\mathcal{G})=\omega} (-\lambda)^{V_t(\mathcal{G})}\Big(-\frac{\lambda_p}{3}\Big)^{V_p(\mathcal{G})}(-\lambda_d)^{V_d(\mathcal{G})} C^{2[V_t(\mathcal{G})+V_p(\mathcal{G})+V_d(\mathcal{G})]+1}. \quad (3.25)$$

At leading order one obtains only *melon-tadpole* graphs (see Appendix A for details). Similarly, to the melonic graphs, the melon tadpole graphs can be seen as a truncation of the self energy depicted in Figure 7.

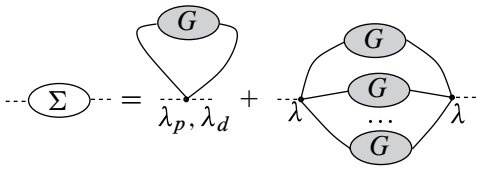

Figure 7. The melon-tadpole self energy.

In the melon-tadpole truncation one includes two graphs. The first one is a tadpole graph whose vertex is either a pillow or the double trace such that the edge closes the

maximal number of faces. The second is a melon with two tetrahedral vertices. At leading order, we have

$$(G^{\mathrm{LO}})^{-1} = C^{-1} - \Sigma^{\mathrm{LO}}, \quad \Sigma^{\mathrm{LO}} = -(\lambda_p + \lambda_d)G^{\mathrm{LO}} + \lambda^2 (G^{\mathrm{LO}})^3. \tag{3.26}$$

4. The 2PI formalism

It is often convenient to recast a QFT in terms of an effective action [24,64]. Effective actions integrate out the quantum fluctuations and the correlation functions are computed by functional derivatives. The most familiar case is the one particle irreducible (1PI) effective action, but the concept is directly generalized to p particle irreducible effective actions [64].

Unsurprisingly, in practice the effective actions are very difficult to compute and one needs to resort to truncations. The situation is greatly simplified in the case of vector models. The two particle irreducible (2PI) action is particularly well suited for their study because it can be explicitly computed order by order in the $1/N$ expansion [11]. It turns out that tensor models are similar [8], and the 2PI action can be computed explicitly at first orders in $1/N$. However, contrary to the vector case, for tensors the effective action is non-local at leading order which leads to much richer physics.

4.1. The 2PI effective action

We introduce some more notation, to be used only in this section. We denote functionals by bold letters and functions by straight letters. We denote the field by ϕ_x, where x denotes the position and any additional indices. Repeated indices are summed/integrated. Bilocal fields are denoted by G_{xy}, J_{xy}, and so on. A dot denotes integrals and index contractions. We will sometimes suppress the indices to simplify the notation.

We consider a scalar theory with action and partition function:

$$\boldsymbol{S}[\phi] = \frac{1}{2}\phi \cdot C^{-1} \cdot \phi + \boldsymbol{S}^{\mathrm{int}}[\phi], \quad \mathcal{Z} = \int [d\phi] e^{-\boldsymbol{S}[\phi]}. \tag{4.1}$$

The interaction part of the action $\boldsymbol{S}^{\mathrm{int}}[\phi]$ can include bivalent vertices. They will always be treated as a perturbation of the free theory defined by the covariance C. In addition, we require the one point function of the theory to be zero

$$\langle \phi_x \rangle = \mathcal{Z}^{-1} \int [d\phi] e^{-\boldsymbol{S}[\phi]} \phi_x = 0.$$

This is guaranteed if the action is even $\boldsymbol{S}[-\phi] = \boldsymbol{S}[\phi]$, which we will assume from now on. Note however that for a colored model the one point function is zero in any rank, even though the action is even only for odd rank.

In order to define the effective action [8, 9], we start from the generating function with bilocal source term J_{xy}:

$$e^{\boldsymbol{W}[J]} = \int [d\phi] e^{-\boldsymbol{S}[\phi]+\frac{1}{2}\phi\cdot J\cdot\phi}. \tag{4.2}$$

Observe that, even in the presence of the source, the odd point expectations are zero. The functional $\boldsymbol{W}[J]$ can either be seen as a generating function of connected moments with a bilocal source, or as the free energy of the theory with shifted covariance $C^{-1} - J$. It includes the ring graph consisting in only an edge closing onto itself whose amplitude[13] is $-\frac{1}{2}\operatorname{Tr}\ln[C^{-1} - J]$.

The derivatives of $\boldsymbol{W}$ are[14]

$$\begin{aligned} 2\frac{\delta \boldsymbol{W}}{\delta J_{xy}} &= \langle \phi_x \phi_y \rangle^J = \langle \phi_x \phi_y \rangle_c^J \equiv \boldsymbol{G}_{xy}, \\ 4\frac{\delta^2 \boldsymbol{W}}{\delta J_{xy} \delta J_{ab}} &= \langle \phi_x \phi_y \phi_a \phi_b \rangle^J - \langle \phi_x \phi_y \rangle^J \langle \phi_a \phi_b \rangle^J \\ &= \langle \phi_x \phi_y \phi_a \phi_b \rangle_c^J + \boldsymbol{G}_{xa}\boldsymbol{G}_{yb} + \boldsymbol{G}_{xb}\boldsymbol{G}_{ya}, \end{aligned} \tag{4.3}$$

where the upper script J signifies that correlations are computed in the presence of the bilocal source J. The functional $\boldsymbol{G}_{xy}$ (which is a functional of the source J) is the connected two point function of the theory with source J. Note that the second derivative of $\boldsymbol{W}$ is exactly the four point function $\langle \phi_x \phi_y \phi_a \phi_b \rangle^J_{(xy)\to(ab)}$ we encountered in Section 2. Going "on shell" means putting the source $J = 0$.

We denote by $\boldsymbol{J}[G]$ the inverse functional of $\boldsymbol{G}[J]$, that is the solution of the equation $\boldsymbol{G}[J] = G$. The effective action is the Legendre transform of $\boldsymbol{W}$ with respect to J:

$$\boldsymbol{\Gamma}[G] = -\boldsymbol{W}[\boldsymbol{J}] + \frac{1}{2}\operatorname{Tr}[G\boldsymbol{J}], \tag{4.4a}$$

$$\frac{\delta \boldsymbol{\Gamma}}{\delta G_{xy}} = \frac{1}{2}\boldsymbol{J}_{xy}, \tag{4.4b}$$

$$\frac{\delta^2 \boldsymbol{\Gamma}}{\delta G_{ab}\delta G_{xy}} = \frac{1}{2}\frac{\delta \boldsymbol{J}}{\delta G} = \frac{1}{2}\Big(\frac{\delta \boldsymbol{G}}{\delta J}\Big)^{-1}_{J=\boldsymbol{J}} = \frac{1}{4}\Big(\frac{\delta^2 \boldsymbol{W}}{\delta J_{xy}\delta J_{ab}}\Big)^{-1}_{J=\boldsymbol{J}}. \tag{4.4c}$$

[13] We normalized the integral to 1 for $\boldsymbol{S}^{\text{int}} = 0, J = 0, C = 1$.

[14] For symmetric functions the derivative is the symmetric projector

$$\frac{\delta J_{xy}}{\delta_{J_{ab}}} = \frac{1}{2}(\delta_{xa}\delta_{yb} + \delta_{xb}\delta_{ya}) \equiv \mathcal{S}_{xy;ab}.$$

This Legendre transform can be written as a functional integral for ϕ with inverse covariance $C^{-1} - \boldsymbol{J}$ and interaction $\boldsymbol{S}^{\text{int}}[\phi]$:

$$e^{-\boldsymbol{\Gamma}[G]} = e^{-\frac{1}{2}\text{Tr}[G\boldsymbol{J}]} \int [d\phi] e^{-\frac{1}{2}\phi\cdot(C^{-1}-\boldsymbol{J})\cdot\phi - \boldsymbol{S}^{\text{int}}[\phi]}, \tag{4.5}$$

where $\boldsymbol{J}[G]$ is fixed by the condition $\langle\phi\phi\rangle_c^{\boldsymbol{J}} = G$.

We denote by $-\boldsymbol{\Gamma}^{2\text{PI}}[G]$ the generating function of nontrivial 2PI graphs (that is graphs which do not disconnect when cutting two edges) with propagator G and vertices in $\boldsymbol{S}^{\text{int}}[\phi]$. If $\boldsymbol{S}^{\text{int}}[\phi]$ has bivalent vertices, $\boldsymbol{\Gamma}^{2\text{PI}}[G]$ contains the graph formed by only one edge with propagator G connected on the bivalent vertex. For example, in zero dimension with $\boldsymbol{S}^{\text{int}}[\phi] = \frac{m^2}{2}\phi^2 + \frac{\lambda}{4!}\phi^4$ we have

$$\boldsymbol{\Gamma}^{2\text{PI}}[G] = \frac{m^2}{2}G + \frac{\lambda}{4!}3G^2 - \frac{1}{2}\Big(\frac{\lambda}{4!}\Big)^2 4!G^4 + \mathcal{O}(\lambda^3). \tag{4.6}$$

The associated graphs are depicted in Figure 8. Observe that the mass vertex appears in only one 2PI graph.

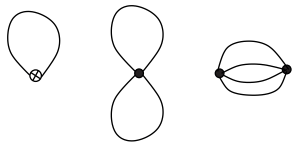

Figure 8. Graphs contributing to the 2PI action at first orders in a ϕ^4 theory.

The derivatives of the 2PI generating function are denoted by

$$\boldsymbol{\Sigma}[G]_{xy} = -2\frac{\delta\boldsymbol{\Gamma}^{2\text{PI}}}{\delta G_{xy}}, \quad \boldsymbol{K}[G]_{ab;xy} = G_{aa'}G_{bb'}\frac{\delta\boldsymbol{\Sigma}_{xy}}{\delta G_{a'b'}}. \tag{4.7}$$

Here, $\boldsymbol{\Sigma}$ is the *self energy* (the amputated one particle irreducible two point function) expressed in terms of the full two point function G. To see this we observe that the derivative cuts an edge and 2 counts the ways to attach it to the external end points. The fact that this is nothing but the self energy in which all the propagators are fully dressed comes from the remark that the configuration depicted on the left in Figure 9 is excluded by the two particle irreducibly condition.

The kernel $\boldsymbol{K}$ is the *irreducible four point kernel* in the channel $(ab) \to (xy)$. As it comes from a derivative of $\boldsymbol{\Sigma}$, it can not contain two edges which, when cut, disconnect the kernel into a component having the external points a, b and another component having the external points x, y (this is depicted in Figure 9 in the middle). However, the kernel $\boldsymbol{K}$ can be disconnected by cutting two edges in a different channel.

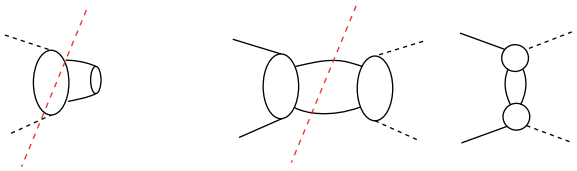

Figure 9. Left: a two particle reducible contribution to the self energy. Right: two contributions to the four point kernel, one which is two particle reducible in the channel $(ab) \to (cd)$ and one which is not (although it is two particle reducible in a different channel. Solid lines represent full two point functions G while dashed lines represent amputations.

For any source J, the two point function is determined self consistently by the Schwinger–Dyson equation:

$$G^{-1} = C^{-1} - J - \mathbf{\Sigma}[G]. \tag{4.8}$$

This equation fixes the source $\boldsymbol{J}[G] = C^{-1} - G^{-1} - \mathbf{\Sigma}[G]$ which ensures that the two point function is exactly G. In particular,

$$\frac{\delta \mathbf{\Gamma}}{\delta G} = \frac{1}{2}\boldsymbol{J} = \frac{1}{2}C^{-1} - \frac{1}{2}G^{-1} - \frac{1}{2}\mathbf{\Sigma}[G], \tag{4.9}$$

and, recalling that the self energy is the derivative of the 2PI generating function, this equation can be integrated to obtain[15]

$$\mathbf{\Gamma}[G] = \frac{1}{2}\operatorname{Tr}\left[C^{-1}G\right] - \frac{1}{2}\operatorname{Tr}[\ln(G)] + \mathbf{\Gamma}^{\text{2PI}}[G]. \tag{4.10}$$

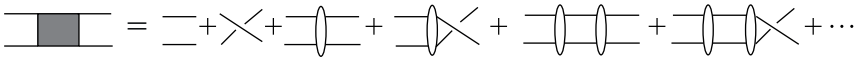

Figure 10. The four point Dyson equation.

The second derivative of $\mathbf{\Gamma}$ is related to the four point kernel:

$$\frac{\delta^2 \mathbf{\Gamma}}{\delta G_{ab}\delta G_{xy}} = \frac{1}{2}G^{-1}_{aa'}G^{-1}_{bb'}(\mathcal{S} - \boldsymbol{K})_{a'b';xy}. \tag{4.11}$$

[15] It is sometimes useful to give a formal functional integral formula for $\mathbf{\Gamma}$

$$e^{-\mathbf{\Gamma}[G]} = e^{-\frac{1}{2}\operatorname{Tr}[C^{-1}G]} \int_{\text{2PI}} [d\phi] e^{-\frac{1}{2}\phi\cdot G^{-1}\phi - \boldsymbol{S}^{\text{int}}[\phi]}.$$

Combining this with (4.4) and (4.3), we find the Dyson equation (see Figure 10) of the four point function connecting (ab) to (xy):

$$\langle \phi_x \phi_y \phi_a \phi_b \rangle^{\boldsymbol{J}}_{(ab)\to(xy)} = \Big(\frac{1}{1-\boldsymbol{K}}\Big)_{ab;x'y'} (G_{x'x} G_{y'y} + G_{x'y} G_{y'x}). \tag{4.12}$$

The correlation functions of the original theory are recovered by taking derivatives of $\boldsymbol{\Gamma}$ and then going on shell, that is setting the two point function to be G^0, the solution of

$$\boldsymbol{J}[G^0] = 0 = C^{-1} - (G^0)^{-1} - \boldsymbol{\Sigma}[G^0]. \tag{4.13}$$

4.2. The Bethe Salpeter equation

Let $O_{\bar{\mu};x}$ be a local operator with some spin:

$$[\partial_{\mu_1 \dots \mu_{j_1}} (-\partial^2)^{n_1} \phi_x][\partial_{\mu_{j_1+1} \dots \mu_{j_1+j_2}} (-\partial^2)^{n_2} \phi_x] \dots \\ [\partial_{\mu_{j_{q-1}+1} \dots \mu_{j_{r-1}+j_r}} (-\partial^2)^{n_r} \phi_x]. \tag{4.14}$$

We aim to find a closed equation for $\langle \phi_{x_1} \phi_{x_2} O_{\bar{\mu};x} \rangle_c$, the three point connected function. To this end we define the generating function with a source $\varepsilon^{\bar{\mu}}_x$ for our operator:

$$e^{\boldsymbol{W}^{\varepsilon}[J]} = \int [d\phi] e^{-\boldsymbol{S}[\phi] + \frac{1}{2}\phi \cdot \boldsymbol{J} \cdot \phi + \varepsilon^{\bar{\mu}} \cdot O_{\bar{\mu}}}, \tag{4.15}$$

We assume that the one point expectation $\langle \phi_x \rangle$ is zero in the presence of the source. This is always the case if O contains an even number of fields ϕ. Then,

$$\langle O_{\bar{\mu};x} \rangle^{J,\varepsilon}_c = \langle O_{\bar{\mu};x} \rangle^{J,\varepsilon} = \frac{\delta \boldsymbol{W}^{\varepsilon}}{\delta \varepsilon^{\bar{\mu}}_x}, \tag{4.16a}$$

$$\begin{aligned} \langle \phi_{x_1} \phi_{x_2} O_{\bar{\mu};x} \rangle^{J,\varepsilon}_c &= \langle \phi_{x_1} \phi_{x_2} O_{\bar{\mu};x} \rangle^{J,\varepsilon} - \langle \phi_{x_1} \phi_{x_2} \rangle^{J,\varepsilon}_c \langle O_{\bar{\mu};x} \rangle^{J,\varepsilon}_c \\ &= 2 \frac{\delta^2 \boldsymbol{W}^{\varepsilon}}{\delta J_{x_1 x_2} \delta \varepsilon^{\bar{\mu}}_x}. \end{aligned} \tag{4.16b}$$

The physical expectations in the theory are obtained by going on shell $J = 0$ and setting the source $\varepsilon = 0$. The results of the previous section go through, except that everything now depends on the source ε. We have

$$2 \frac{\delta \boldsymbol{W}^{\varepsilon}}{\delta J_{x_1 x_2}} = \boldsymbol{G}^{\varepsilon}[J]_{x_1 x_2}, \quad \frac{\delta \boldsymbol{G}^{\varepsilon}_{x_1 x_2}}{\delta \varepsilon^{\bar{\mu}}_x} = \langle \phi_{x_1} \phi_{x_2} O_{\bar{\mu};x} \rangle^{J,\varepsilon}_c, \tag{4.17}$$

and we denote by $\boldsymbol{J}^{\varepsilon}[G]$ the inverse functional of $\boldsymbol{G}^{\varepsilon}[J]$ and the Legendre transform of $\boldsymbol{W}^{\varepsilon}[J]$ by

$$\boldsymbol{\Gamma}^{\varepsilon}[G] = -\boldsymbol{W}^{\varepsilon}[\boldsymbol{J}^{\varepsilon}] + \frac{1}{2} \operatorname{Tr}[G \boldsymbol{J}^{\varepsilon}], \tag{4.18a}$$

$$\boldsymbol{\Gamma}^{\varepsilon}[G] = \frac{1}{2} \operatorname{Tr}\big[C^{-1} G\big] - \frac{1}{2} \operatorname{Tr}[\ln(G)] + \boldsymbol{\Gamma}^{2\mathrm{PI};\varepsilon}[G]. \tag{4.18b}$$

The functional $-\mathbf{\Gamma}\,2\mathrm{PI};\varepsilon[G]$ is now the sum over 2PI graphs (from the point of view of ϕ) with propagator G and vertices in $\boldsymbol{S}^{\mathrm{int}}[\phi]$ or $\varepsilon\cdot O$. With respect to the previous case, we now have additional vertices with coordination r representing insertions of the operator O in the graphs. The derivatives of $\mathbf{\Gamma}^{\varepsilon}$ can be computed using either the Legendre transform or the explicit formula relating $\mathbf{\Gamma}^{\varepsilon}$ to $\mathbf{\Gamma}\,2\mathrm{PI};\varepsilon$. In particular,

$$-2\frac{\delta\mathbf{\Gamma}^{\varepsilon}}{\delta G_{x_1x_2}\delta\varepsilon^{\bar{\mu}}_{x}}=-2\frac{\delta}{\delta\varepsilon^{\bar{\mu}}_{x}}\Big(\frac{\delta\mathbf{\Gamma}^{\varepsilon}}{\delta G_{x_1x_2}}\Big)=-\frac{\delta\boldsymbol{J}^{\varepsilon}_{x_1x_2}}{\delta\varepsilon^{\bar{\mu}}_{x}}[G], \tag{4.19a}$$

$$-2\frac{\delta\mathbf{\Gamma}^{\varepsilon}}{\delta G_{x_1x_2}\delta\varepsilon_{x}}=-2\frac{\delta\mathbf{\Gamma}^{2\mathrm{PI};\,\varepsilon}}{\delta G_{x_1x_2}\delta\varepsilon^{\bar{\mu}}_{x}}\equiv\langle\phi_{x_1}\phi_{x_2}O_{\bar{\mu};x}\rangle^{\boldsymbol{J}^{\varepsilon},\varepsilon}_{2\mathrm{PI}}. \tag{4.19b}$$

The last correlation $\langle\phi_{x_1}\phi_{x_2}O_{\bar{\mu};x}\rangle^{G;\varepsilon}_{2\mathrm{PI}}$ is represented in Figure 11. It is two particle irreducible in the channel $(\phi\phi)\to O$, that is by cutting two edges it can not be disconnected in a component containing both external points ϕ and a second connected component containing the operator O.

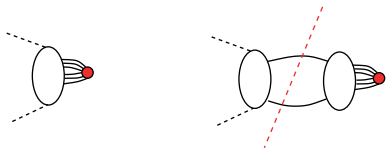

Figure 11. On the left the correlation function $\langle\phi_{x_1}\phi_{x_2}O_{\bar{\mu};x}\rangle^{G;\varepsilon}_{2\mathrm{PI}}$. On the right a contribution which is two particle reducible in the channel $(\phi\phi)\to O$. The red dot represents the composite operator.

On the other, by definition $\boldsymbol{G}^{\varepsilon}[\boldsymbol{J}^{\varepsilon}[G]]=G$; therefore

$$\begin{aligned}0&=\frac{\delta\boldsymbol{G}^{\varepsilon}_{x_1x_2}}{\delta\varepsilon^{\bar{\mu}}_{x}}\Big|_{J=\boldsymbol{J}^{\varepsilon}}+\frac{\delta\boldsymbol{G}^{\varepsilon}_{x_1x_2}}{J_{ab}}\Big|_{J=\boldsymbol{J}^{\varepsilon}}\frac{\delta\boldsymbol{J}^{\varepsilon}_{ab}}{\delta\varepsilon^{\bar{\mu}}_{x}}\\ \Longrightarrow\quad\frac{\delta\boldsymbol{J}^{\varepsilon}_{ab}}{\delta\varepsilon^{\bar{\mu}}_{x}}&=-2\frac{\delta^2\mathbf{\Gamma}^{\varepsilon}}{\delta G_{ab}\delta G_{uv}}\frac{\delta\boldsymbol{G}^{\varepsilon}_{uv}}{\delta\varepsilon^{\bar{\mu}}_{x}}\Big|_{J=\boldsymbol{J}^{\varepsilon}}.\end{aligned} \tag{4.20}$$

Putting everything together, we conclude that

$$\begin{aligned}\langle\phi_{x_1}\phi_{x_2}O_{\bar{\mu};x}\rangle^{\boldsymbol{J}^{\varepsilon},\varepsilon}_{2\mathrm{PI}}&=2\frac{\delta^2\mathbf{\Gamma}^{\varepsilon}}{\delta G_{x_1x_2}\delta G_{uv}}\frac{\delta\boldsymbol{G}^{\varepsilon}_{uv}}{\delta\varepsilon^{\bar{\mu}}_{x}}\Big|_{J=\boldsymbol{J}^{\varepsilon}}\\&=G^{-1}_{x_1a}G^{-1}_{x_2b}(\mathcal{S}-\boldsymbol{K}^{\varepsilon})_{ab;uv}\langle\phi_u\phi_v O_{\bar{\mu};x}\rangle^{\boldsymbol{J}^{\varepsilon},\varepsilon}_{c},\end{aligned} \tag{4.21}$$

which can be rewritten, taking $\varepsilon=0$, in the form

$$\langle\phi_{x_1}\phi_{x_2}O_{\bar{\mu};x}\rangle^{\boldsymbol{J}}_{c}=G_{x_1a}G_{x_2b}\langle\phi_a\phi_b O_{\bar{\mu};x}\rangle^{\boldsymbol{J}}_{2\mathrm{PI}}+\boldsymbol{K}_{x_1x_2;ab}\langle\phi_a\phi_b O_{\bar{\mu};x}\rangle^{\boldsymbol{J}}_{c}. \tag{4.22}$$

This equation should be compared with (2.22):

$$\int dx_3^d dx_4^d K(x_1, x_2; x_3, x_4) \langle \phi(x_3)\phi(x_4) O^{\bar{\mu}}_{\Delta,J}(x)\rangle = k(\Delta, J)\langle \phi(x_1)\phi(x_2) O^{\bar{\mu}}_{\Delta,J}(x)\rangle, \tag{4.23}$$

together with the condition that the physical primary operators are such that

$$k(\Delta, J) = 1.$$

This means that in a CFT the 2PI contribution to the three point function of two ϕ fields and a primary $O_{\bar{\mu}}$ must be identically zero. The implications of this fact need to be investigated in depth.

4.3. The $1/N$ expansion and melonic theories

We consider the generalization of the $O(N)^3$ model to dimension d. We use the notation of Section 3. The field is a tensor with three indices $\phi_A(x)$ and the action of the $O(N)^3$ field theory is

$$\begin{aligned} S[\phi] = &\frac{1}{2}\int_{xy} \phi_A(x)(C^{-1})(x,y)\phi_A(y) + \frac{1}{2}m\int_x \phi_A(x)\phi_A(x) \\ &+ \int_x \Big(\frac{\lambda}{4N^{3/2}}\delta^t_{ABCD} + \frac{\lambda_p}{4N^2}\delta^p_{AB;CD} + \frac{\lambda_d}{4N^3}\Big)\phi_A(x)\phi_B(x)\phi_C(x)\phi_D(x), \end{aligned} \tag{4.24}$$

where from now on we reinstate the separation between the position arguments and the tensor indices. We added a mass parameter m and the covariance of the theory, C, is kept arbitrary for now.

The source $J_{AB}(x, y)$ is bilocal both in positions and tensor indices. In order to determine the scaling in N of a term in the 2PI action, we use the diagonal ansatz $G_{AB}(x, y) \sim \delta_{AB} G(x, y)$ because on shell the two point function is indeed diagonal in the tensor indices. It follows that the scaling in N of the 2PI graphs is just the standard scaling in N discussed in Section 3. At leading order only melon–tadpole graphs contribute, and the only 2PI melon–tadpole graphs are those represented in Figure 8. This is because an insertion of a melon or a tadpole in any of the three graphs yields a two particle reducible contribution. At leading order in $1/N$ we get

$$\begin{aligned} \mathbf{\Gamma}^{2\mathrm{PI}}[G] = &\frac{m}{2}\mathrm{Tr}[G] + \int_x G_{AB}(x,x)\Big(\frac{\lambda_p}{4N^2}\delta^p_{AB;CD} + \frac{\lambda_d}{4N^3}\delta^d_{AB;CD}\Big)G_{CD}(x,x) \\ &- \frac{1}{2}\Big(\frac{\lambda}{4N^{3/2}}\Big)^2 4\int_{x,y} \delta^t_{A_1A_2A_3A_4}\delta^t_{B_1B_2B_3B_4}\prod_i G_{A_iB_i}(x,y). \end{aligned} \tag{4.25}$$

The self energy is then

$$\begin{aligned}\mathbf{\Sigma}[G]_{AB}(x,y) = &-m\delta_{AB}\delta_{xy}\\ &-\Big(\frac{\lambda_p}{N^2}\delta^p_{AB;CD}+\frac{\lambda_d}{N^3}\delta^d_{AB;CD}\Big)\delta_{xy}G_{CD}(x,x)\\ &+\frac{\lambda^2}{N^3}\delta^t_{AA_1A_2A_3}\delta^t_{BB_1B_2B_3}\prod_{i=1}^{3}G_{A_iB_i}(x,y),\end{aligned} \tag{4.26}$$

and the irreducible kernel is

$$\begin{aligned}&\boldsymbol{K}_{A'B';CD}(x'y';zt)\\ &\quad=G_{A'A}(x',x)G_{B'B}(y',y)\\ &\qquad\times\Big[-\Big(\frac{\lambda_p}{N^2}\delta^p_{AB;CD}+\frac{\lambda_d}{N^3}\delta^d_{AB;CD}\Big)\delta_{xy}\delta_{xz}\delta_{xt}\\ &\qquad\quad+\frac{\lambda^2}{N^3}\delta^t_{AA_1A_2A_3}\delta^t_{BB_1B_2B_3}\\ &\qquad\quad\times\sum_{i=1}^{3}\Big(\frac{1}{2}\delta_{xz}\delta_{yt}\delta_{A_iC}\delta_{B_iD}+\frac{1}{2}\delta_{xt}\delta_{yz}\delta_{A_iD}\delta_{B_iC}\Big)\prod_{j\neq i}G_{C_jD_j}(x,y)\Big].\end{aligned} \tag{4.27}$$

5. Renormalization in a tensor field theory

In Sections 2 and 3 we have seen that melonic CFTs can be analytically treated and that in many models the melonic limit can be recovered as a large N limit. CFTs should correspond to fixed points of the renormalization group and infrared fixed points are especially interesting because they describe the low energy behavior of theories.

The natural question is: are there examples of field theories with infrared attractive fixed points described by melonic CFTs? The answer to this question is yes: many fermionic models in less than 2 dimensions [6, 67, 68, 83, 91, 108], and some supersymmetric [90] or bosonic ones [38] in dimension strictly less that 3 do have melonic infrared fixed points.

However, it turns out that it is not so easy to find models with melonic fixed points in $d = 3$ dimensions. In this section we discuss one example which works [9].

From now on, we consider $d < 4$ dimensions. Although we keep d generic, we are especially interested in the $d = 3$ case. Our starting point is the $O(N)^3$ field theory

described in Section 4, with a suitable covariance:

$$\begin{aligned} S[\phi] = &\frac{1}{2}\int d^d x \phi_A(x)(-\partial^2)^\zeta \phi_A(x) + \frac{1}{2} m \int d^d x \phi_A(x)\phi_A(x) \\ &+ \int d^d x \Big(\frac{\lambda}{4N^{3/2}} \delta^t_{ABCD} \\ &\qquad + \frac{\lambda_p}{4N^2}\delta^p_{AB;CD} + \frac{\lambda_d}{4N^3}\Big)\phi_A(x)\phi_B(x)\phi_C(x)\phi_D(x), \end{aligned} \tag{5.1}$$

where for now ζ is not fixed and we take the large N limit.

The first choice that comes to mind [39] is $\zeta = 1$, that is the tensor generalization of the standard ϕ^4_4 theory. The quartic couplings are classically marginal in dimension $d = 4$, and one can search for Wilson Fisher [105] like fixed point in $d = 4 - \varepsilon$ dimensions [39]. At first orders one finds the beta functions (where $\tilde{g} = g/(4\pi)^2$)

$$\beta_{\tilde{g}} = -\varepsilon \tilde{g} + 2\tilde{g}^3, \tag{5.2a}$$

$$\beta_{\tilde{g}_p} = -\varepsilon \tilde{g}_p + \Big(6\tilde{g}^2 + \frac{2}{3}\tilde{g}_p^2\Big) - 2\tilde{g}^2\tilde{g}_p, \tag{5.2b}$$

$$\beta_{\tilde{g}_d} = -\varepsilon \tilde{g}_d + \Big(\frac{4}{3}\tilde{g}_p^2 + 4\tilde{g}_p\tilde{g}_d + 2\tilde{g}_d^2\Big) - 2\tilde{g}^2(4\tilde{g}_p + 5\tilde{g}_d), \tag{5.2c}$$

which admit a fixed point

$$g_\star = (\varepsilon/2)^{1/2}, \quad g_{p,\star} = \pm 3\,\mathrm{i}(\varepsilon/2)^{1/2}, \quad g_{d,\star} = \mp\,\mathrm{i}(3 \pm \sqrt{3})(\varepsilon/2)^{1/2}.$$

The pillow and double trace couplings are purely imaginary at the fixed point. This in itself is not a problem, but a more careful study reveals other unpleasant features of the fixed point: searching for the dimensions of the physical primary fields at this fixed point along the lines of Section 2, one finds a primary with complex dimension $d/2 \pm \mathrm{i}\,\alpha$, see [38]. Now, this is problematic.

• In an AdS/CFT picture [48, 107], bulk fields with mass m_{AdS} corresponds to boundary single trace primaries with dimensions $\Delta = d/2 \pm (d^2/4 + m^2_{\mathrm{AdS}})^{1/2}$. Primaries with dimensions $d/2 \pm \mathrm{i}\,\alpha$ correspond to fields with $m^2_{\mathrm{AdS}} < -d^2/4$ violating the Breitenlohner–Freedman bound [15].

• A physical primary with dimension $d/2 \pm \mathrm{i}\,\alpha$ represents a pole of the density $\rho(\Delta, J)$ located exactly on the original contour of integration of the partial waves (recall Section 2). The initial expansion of the four point function in terms of partial waves needs to be revisited in order to deal with this singularity.

• The problematic primary is the mass operator. A dimension of a mass–like primary operator of the form $d/2 \pm \mathrm{i}\,\alpha$ has recently been shown in a similar model [65] to correspond to an instability and signal that the corresponding operator acquires a non-zero vacuum expectation value.

• The dimension of the mass is half the one of the double trace invariant [47] which is $d + \nu$, with ν the critical exponent of the double trace coupling. The dimension $d/2 \pm \mathrm{i}\,\alpha$ of the mass implies that the double trace coupling has a purely imaginary critical exponent. The fixed point is a limit cycle, not an infrared fixed point (see Appendix B).

In $4 + \varepsilon$ dimensions the problem goes away, but the fixed point turns out to be an ultraviolet fixed point: the pillow and double trace couplings are relevant at the fixed point.

In order to find a genuine infrared fixed point described by a melonic CFT, one needs to take a more drastic approach. According to (2.33), in the melonic limit the field is expected to acquire the infrared scaling dimension $\Delta_\phi = d/q$, with $q = 4$ in our case. The idea [9] is to modify the ultraviolet scaling of the free part of the action ζ in such a way that the UV scaling dimension of the field $(d - 2\zeta)/2$ equals the IR one.

From now on, we fix $\zeta = d/2 - d/q$, which is $\zeta = d/4$ for $q = 4$. This means that the free part of the action has a non-integer power of the momentum. Before continuing, let us briefly comment on this. Although models with non-integer scaling have been considered in the literature [1, 18] (and more recently in [44] in the context of the SYK model), they might be somewhat unfamiliar to the reader.

For any $\zeta \leq 1$ the free theory,

$$\boldsymbol{S}_0[\phi] = \frac{1}{2}\int d^d x \phi(x)(-\partial^2)^\zeta \phi(x), \quad \zeta \leq 1, \tag{5.3}$$

is *unitary* because it is explicitly Osterwalder Schrader positive. Indeed, the covariance

$$C(p) = \frac{1}{p^{2\zeta}} = \frac{1}{\Gamma(\zeta)}\int_0^\infty d\alpha \alpha^{\zeta-1} e^{-\alpha p^2}, \tag{5.4a}$$

$$\begin{aligned} C(x-y) &= \frac{1}{(4\pi)^{d/2}\Gamma(\zeta)}\int_0^\infty d\alpha \alpha^{\zeta-1-d/2} e^{-\frac{(x-y)^2}{4\alpha}} \\ &= \frac{\Gamma\left(\frac{d}{2}-\zeta\right)}{2^{2\zeta}\pi^{d/2}\Gamma(\zeta)}\frac{1}{|x-y|^{d-2\zeta}}, \end{aligned} \tag{5.4b}$$

(where the last equality holds for $d - 2\zeta > 0$) admits an absolutely convergent Källén–Lehmann spectral representation as a superposition of massive particles with a continuous mass spectrum:

$$\frac{1}{p^{2\zeta}} = \frac{1}{\Gamma(\zeta)\Gamma(1-\zeta)}\int_0^\infty dx \frac{x^{-\zeta}}{p^2 + x}. \tag{5.5}$$

The condition $\zeta < 1$ is crucial for the convergence in 0.

One can also consider interacting theories with $\zeta < 1$, see [1, 18]. The most well-known example is the Brydges–Mitter–Scoppola model with $d = 3$, $\zeta = 3/4 + \varepsilon$ and $\lambda\phi^4$ interaction. This model has

- the Gaussian fixed point where the quartic coupling is relevant,
- an interacting fixed point $g_\star \sim \varepsilon$ (with g the running dimensionless quartic coupling) where the quartic coupling is irrelevant,
- a renormalization group trajectory connecting the two fixed points.

These statements can are rigorously proven [1, 18]. The infrared fixed point of this model is the inspiration for using a non-integer scaling in our case.

5.1. Renormalization

Although q is fixed to 4, we will often keep it generic. There are two reasons for this. First, this makes the comparison with Section 2 easier. Second, it is likely that some of the results can be generalized for colored models with q body interactions. As $\zeta = d/2 - d/q$ and $\zeta < 1$, we obtain a bound $d < 2q/(q-2)$, that is,

- for $q = 4$, $d < 4$ (in particular, this covers a quartic model in $d = 3$, our main interest; the case $4 - \varepsilon$ can also be recovered);
- for $q = 6$, $d < 3$;
- any q in $d = 2$.

Following Appendix B, we introduce both an ultraviolet cutoff Λ and an infrared cutoff k:

$$C_k^\Lambda = \frac{1}{p^{2\zeta}} \chi_k^\Lambda(p) = \frac{1}{\Gamma(\zeta)} \int_{\Lambda^{-2}}^{k^{-2}} d\alpha \alpha^{\zeta-1} e^{-\alpha p^2}, \tag{5.6}$$

that is, we chose a multiplicative cutoff

$$\Theta(u) = \Gamma(\zeta)^{-1} \int_u^\infty d\alpha \alpha^{\zeta-1} e^{-\alpha}$$

which is an upper incomplete Euler Gamma function. We aim to compute the wave function renormalization (and consequently the anomalous field dimension) and the β functions of the couplings.

We start from the large N self energy and four point kernel. Using Section 4, on shell we have $G_{AB}(x,y) = G_{xy}\delta_{AB}$ and

$$\Sigma_{AB}(x,y) = \delta_{AB}\Sigma_{xy}, \tag{5.7a}$$

$$\Sigma_{xy} = -m\delta_{xy} - (\lambda_p + \lambda_d)\delta_{xy}G_{xx} + \lambda^2 G_{xy}^3, \tag{5.7b}$$

$$K_{AB;CD}(x'y';zt) = G_{x'x}G_{y'y}\Big[-\frac{\lambda_p}{N^2}\delta^p_{AB;CD}\delta_{xy}\delta_{xz}\delta_{zt} - \frac{\lambda_d}{N^3}\delta^d_{AB;CD}\delta_{xy}\delta_{xz}\delta_{zt} + \frac{\lambda^2}{N^2}3\delta^p_{AB;CD}\delta_{xz}\delta_{yt}G_{xy}^2\Big], \tag{5.7c}$$

where m and λ denote the dimensionful mass parameter and four point couplings at the UV scale Λ. It is convenient to parametrize the interaction in terms of $\lambda_1 = \lambda_p/3$ and $\lambda_2 = \lambda_p + \lambda_d$ and the two mutually orthogonal projectors

$$P_1 = 3\Big(\frac{1}{N^2}\delta^p - \frac{1}{N^3}\delta^d\Big) \quad \text{and} \quad P_2 = \frac{1}{N^3}\delta^d.$$

In momentum space, we get

$$\Sigma(p) = -m - \lambda_2 \int_r G(r) + \lambda^2 \int_{r_1 r_2} G(r_1)G(r_2)G(p + r_1 + r_2) \tag{5.8a}$$

$$K_{p_1,p_2;r_1,r_2} = (2\pi)^d \delta(p_1 + p_2 - r_1 - r_2)G(p_1)G(p_2) \times \Big[\Big(\lambda^2 \int_r G(r)G(r + p_1 - r_1) - \lambda_1\Big)P_1 + \Big(3\lambda^2 \int_r G(r)G(r + p_1 - r_1) - \lambda_2\Big)P_2\Big]. \tag{5.8b}$$

Note that λ_1 is essentially the pillow coupling and λ_2 essentially the double trace one.

The wave function. In momentum space the Schwinger–Dyson equation with cutoffs becomes

$$G_k(p)^{-1} = p^{2\zeta}\chi^{-1} + m + \lambda_2 \int_r G_k(r) - \lambda^2 \int_{r_1 \dots r_{q-2}} G_k(r_1)\dots G_k(r_{q-2})G_k(p + r_1 + \dots + r_q), \tag{5.9}$$

where in the last term we reintroduced a generic q. It turns out that (after tuning the bare mass)

$$G_k(p) = \frac{1}{Zp^{2\zeta}}\chi_k^\Lambda(p), \quad \zeta = \frac{d}{2} - \frac{d}{q}, \tag{5.10}$$

with a constant Z (to be determined below) verifies (5.9) up to terms which vanish in the limit $k \to 0$. The important point is that the total Z is finite, hence the anomalous field dimension $\eta_\star$ is zero. This is consistent with the fact that ζ has been chosen such that the ultraviolet and infrared scaling dimensions of the field coincide.

To check this, let us first consider the local part of the right-hand side of (5.9) (we need to remember that $q = 4$ hence $\zeta = d/4$ for this discussion):

$$m + \lambda_2 \int_r G_k(r) - \lambda^2 \int_{r_1 r_2} G_k(r_1) G_k(r_2) G_k(r_1 + r_2). \tag{5.11}$$

The first term is $\int_r G_k(r) \sim k^{d/2} - \Lambda^{d/2}$, which vanishes in the $k \to 0$ limit if $m = -\lambda_2 \Lambda^{d/2}$. The second term is similar.

Once the local part of the SDE is subtracted via a Taylor expansion with integral rest [9], we can take the cutoffs to their limits and, rescaling the α by p^2, we obtain

$$\begin{aligned} Z p^{2\zeta} =& p^{2\zeta} + p^{2\zeta} \frac{\lambda^2}{(4\pi)^{d\frac{q-2}{2}} \Gamma(\zeta)^{q-1} Z^{q-1}} \\ &\times \int_0^1 dt \int_0^\infty d\alpha \frac{\prod_{i=1}^{q-1} \alpha_i^\zeta}{\left(\sum_{i=1}^{q-1} \prod_{j\neq i} \alpha_j\right)^{d/2+1}} e^{-t \frac{\prod_{i=1}^{q-1} \alpha_i}{\sum_{i=1}^{q-1} \prod_{j\neq i} \alpha_j}}. \end{aligned} \tag{5.12}$$

Using Appendix C, we see that the total wave function renormalization Z verifies the equations

$$1 = \frac{1}{Z} + \frac{1}{g_c^2} \left(\frac{\tilde{\lambda}}{Z^{q/2}} \right)^2, \tag{5.13a}$$

$$\tilde{\lambda} \equiv \frac{\lambda}{(4\pi)^{\frac{d(q-2)}{4}} \Gamma(\zeta)^{q/2}}, \tag{5.13b}$$

$$\frac{1}{g_c^2} = \frac{\Gamma(\zeta)\Gamma(1-\zeta)\Gamma\left(\frac{d}{2} - \zeta\right)^{q-1}}{\zeta \Gamma\left(\frac{d}{2} + \zeta\right)}. \tag{5.13c}$$

It is instructive to compute the two point function in direct space

$$G(x_{12}) = b |x_{12}|^{-2\Delta_\phi}.$$

Taking the Fourier transform and recalling that $\Delta_\phi = d/q$, we obtain that b verifies

$$1 = b \frac{2^{d-2\Delta_\phi} \pi^{d/2} \Gamma(\frac{d}{2} - \Delta_\phi)}{\Gamma(\Delta_\phi)} + \lambda^2 b^q \pi^d \frac{\Gamma\left(1 - \frac{d}{2} + \Delta_\phi\right) \Gamma\left(\frac{d}{2} - \Delta_\phi\right)}{\left(\frac{d}{2} - \Delta_\phi\right) \Gamma(d - \Delta_\phi) \Gamma(\Delta_\phi)}, \tag{5.14}$$

which reproduces (2.33) if one neglects the first term on the right-hand side.

Four point couplings. From now on, we set

$$\tilde{\lambda} \equiv \frac{\lambda}{(4\pi)^{\frac{d(q-2)}{4}}\Gamma(\zeta)^{q/2}}, \quad \tilde{\lambda}_i \equiv \frac{\lambda_i}{(4\pi)^{d/2}\Gamma(\zeta)^2}. \tag{5.15}$$

The classical scaling dimension of an operator $\partial^J \phi^n$ is $J + n\Delta_\phi$; see Appendix B. In our case, $\Delta_\phi = d/q$ and the only classically marginal operators are $J = 0, n = q$. For $q = 4$ they are the tetrahedron, pillow and double trace.

At leading order in $1/N$, the tetrahedral coupling does not receive any radiative correlation therefore the renormalized tetrahedral coupling is just a rescaling of the bare one by the wave function constant. Using the tilde couplings, we write

$$\tilde{g} = \frac{\tilde{\lambda}}{Z^{q/2}}. \tag{5.16}$$

The renormalized tetrahedral coupling does not run, hence it is just a parameter which can be adjusted. On the contrary, the pillow and double trace couplings do run. We denote by $\tilde{g}_1, \tilde{g}_2$ the running dimensionless couplings at scale k (we suppress the dependence in k in order to simplify the notation). We will still keep q generic in some formulae, but we will remember that the pillow and double trace couplings are four point couplings. The $\tilde{g}_i$s are the amputated 1PI four point functions at zero momentum divided by Z^2. In terms of the four point kernel (5.8), we get

$$\tilde{g}_i = \frac{\Gamma^{4;i}}{(4\pi)^{d/2}\Gamma(\zeta)^2 Z^2}, \quad -\Gamma^{4;1}P_1 - \Gamma^{4;2}P_2 = G^{-1}G^{-1}\frac{K}{1-K}. \tag{5.17}$$

As P_1 and P_2 are mutually orthogonal, the two cases $i = 1, 2$ are identical up to substituting $\tilde{\lambda}^2$ by $(q-1)\tilde{\lambda}^2$.

Expanding the series in (5.17), we obtain the bare expansion: $\tilde{g}_1$ is a sum over "sausage graphs" depicted in Figure 12. A sausage graph is a sequence of vertical irreducible pieces connected by pairs of horizontal edges. The vertical pieces are either ladder rungs with two tetrahedral couplings or bare vertices λ_1.

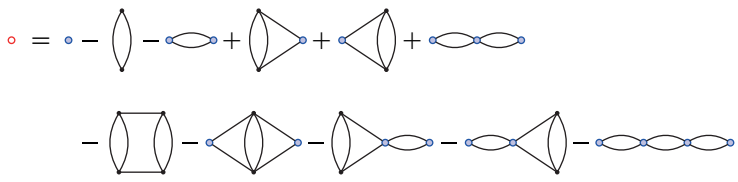

Figure 12. The bare series up to quartic order (the blue vertices represent λ_1).

Each graph has a (log divergent) amplitude:

$$A(\mathcal{G}) = \int_{\Lambda^{-2}}^{k^{-2}} \Big(\prod_{e\in\mathcal{G}} d\alpha_e \alpha_e^{\xi-1}\Big) \frac{1}{\big[\sum_{\mathcal{T}\subset\mathcal{G}} \prod_{e\notin\mathcal{T}} \alpha_e\big]^{d/2}}, \tag{5.18}$$

where $e \in \mathcal{G}$ runs over the edges of $\mathcal{G}$ and $\mathcal{T}$ over the trees in $\mathcal{G}$, see [74, 92]. The graph consisting in only a bare vertex has amplitude 1. We denote by $\mathfrak{S}$ the set of connected sausage graphs with at least two internal vertices, and $n_t(\mathcal{G})$ respectively $n_1(g)$ the numbers of tetrahedral vertices and blue vertices of $\mathcal{G}$. Then,

$$\tilde{g}_1(\tilde{\lambda}_1, \tilde{\lambda}) = \frac{\tilde{\lambda}_1}{Z^2} + \sum_{\mathcal{G}\in\mathfrak{S}} (-1)^{1+n_1(\mathcal{G})} \Big(\frac{\tilde{\lambda}}{Z^{q/2}}\Big)^{n_t(\mathcal{G})} \Big(\frac{\tilde{\lambda}_1}{Z^2}\Big)^{n_1(\mathcal{G})} A(\mathcal{G}). \tag{5.19}$$

Observe that this is naturally a series in the renormalized tetrahedral coupling $\tilde{g} = Z^{-q/2}\tilde{\lambda}$. The bare expansion for g_2 is identical up to replacing $\tilde{\lambda}^2$ by $(q-1)\tilde{\lambda}^2$.

The graphs with no internal λ_1 vertex are special. They might have no external λ_1 vertex either (ladders), or one external λ_1 vertex (caps) or two external λ_1 vertices (double caps), as depicted in Figure 13.

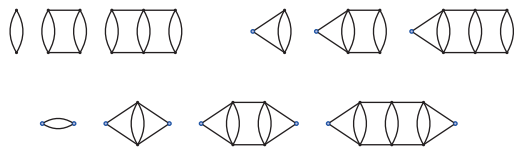

Figure 13. Ladders, caps and double caps.

Let us denote by U_r, S_r, T_r the amplitude of the ladder, cap respectively double cap with $2r$ tetrahedral vertices, and let us define the generating functions:

$$U(\tilde{g}) = \sum_{r\geq 1} \tilde{g}^{2r} U_r, \quad S(\tilde{g}) = \sum_{r\geq 1} \tilde{g}^{2r} S_r, \quad T(\tilde{g}) = \sum_{r\geq 0} \tilde{g}^{2r} T_r, \tag{5.20}$$

where, in $S(\tilde{g})$ and $T(\tilde{g})$, we have *not* included any coupling constants for the λ_1 vertices. The crucial fact is that the amplitude of any sausage factors at the internal λ_1 vertices, thus

$$\tilde{g}_1 = -U(\tilde{g}) + \Big(\frac{\tilde{\lambda}_1}{Z^2}\Big) \frac{[1+S(\tilde{g})]^2}{1+\frac{\tilde{\lambda}_1}{Z^2} T(\tilde{g})}. \tag{5.21}$$

This gives a particularly simple β function and short computation yields

$$\beta_{\tilde{g}_1} = k\partial_k \tilde{g}_1 = \beta_0^{\tilde{g}} - 2\beta_1^{\tilde{g}} \tilde{g}_1 + \beta_2^{\tilde{g}} \tilde{g}_1^2, \tag{5.22}$$

with the coefficients of the β function given by

$$\beta_0^{\tilde{g}} = -k\partial_k U + 2\frac{U}{1+S}k\partial_k S - \frac{U^2}{(1+S)^2}k\partial_k T, \tag{5.23a}$$

$$\beta_2^{\tilde{g}} = -\frac{1}{(1+S)^2}k\partial_k T, \tag{5.23b}$$

$$\beta_1^{\tilde{g}} = -\frac{1}{1+S}k\partial_k S + \frac{U}{(1+S)^2}k\partial_k T. \tag{5.23c}$$

This result is an all order result in the couplings: this is the complete β function at leading order in $1/N$. The important remark is that the β functions are quadratic. The coefficients $\beta_{0,1,2}^{\tilde{g}}$ are series in the tetrahedral coupling $\tilde{g}$. While it is not obvious, they are finite term by term in the limit $k \to 0$, see [9].

5.2. Fixed points

Let us recapitulate where we stand. Starting with the UV scaling $\zeta = d/2 - d/q < 1$, hence field dimension $\Delta_\phi = d/q$, we obtained the following results.

Wave function. Tuning the renormalized mass to zero and lifting the cutoffs, the two-point function is

$$G(p) = \frac{1}{Zp^{2\zeta}}, \quad 1 = \frac{1}{Z} + \frac{\tilde{g}^2}{g_c^2}, \quad \frac{1}{g_c^2} = \frac{\Gamma(\zeta)\Gamma(1-\zeta)\Gamma\left(\frac{d}{2}-\zeta\right)^{q-1}}{\zeta\Gamma\left(\frac{d}{2}+\zeta\right)}, \tag{5.24}$$

that is the anomalous field dimension $\eta_\star$ is 0.

Tetrahedral coupling. The tetrahedral coupling has a finite flow, that is the renormalized coupling is a rescaling of the bare one $\tilde{g} = Z^{-q/2}\tilde{\lambda}$. In particular, we have

$$Z = \left(1 - \frac{\tilde{g}^2}{g_c^2}\right)^{-1}, \quad \lambda = \tilde{g}Z^2. \tag{5.25}$$

There are two cases, depicted in Figure 14: $\tilde{\lambda}$ real and $\tilde{\lambda}$ purely imaginary.

- $\tilde{\lambda}$ (and $\tilde{g}$) real. $\tilde{\lambda}(\tilde{g})$ is invertible to $\tilde{g}(\tilde{\lambda})$ for any $\tilde{\lambda}$ and $g < g_c$.
- $\tilde{\lambda}$ (and $\tilde{g}$) imaginary. $\tilde{\lambda}(\tilde{g})$ is invertible to $\tilde{g}(\tilde{\lambda})$ for $|\lambda| < 3^{3/2}2^{-4}g_c$ and $|g| < 3^{-1/2}g_c$ (the end point of the blue curve in Figure 14.

Pillow and double-trace couplings. At leading order in $1/N$ but at all orders in the couplings, the β functions are

$$\beta_{\tilde{g}_1} = k\partial_k \tilde{g}_1 = \beta_0^{\tilde{g}} - 2\beta_1^{\tilde{g}}\tilde{g}_1 + \beta_2^{\tilde{g}}\tilde{g}_1^2, \tag{5.26a}$$

$$\beta_{\tilde{g}_2} = k\partial_k \tilde{g}_2 = \beta_0^{\sqrt{(q-1)}\tilde{g}} - 2\beta_1^{\sqrt{(q-1)}\tilde{g}}\tilde{g}_2 + \beta_2^{\sqrt{q-1}\tilde{g}}\tilde{g}_2^2, \tag{5.26b}$$

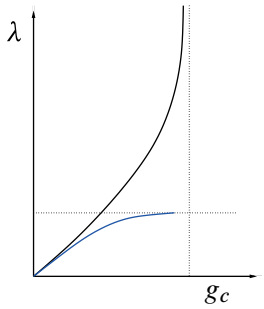

Figure 14. Bare and renormalized tetrahedral couplings (in blue the purely imaginary case).

where $\beta_0^{\tilde{g}}, \beta_1^{\tilde{g}}$ and $\beta_2^{\tilde{g}}$ are power series in $\tilde{g}^2$. At first orders they are [9]

$$\beta_0^{\tilde{g}} = \Big(2\frac{\Gamma\big(\frac{d}{4}\big)^2}{\Gamma\big(\frac{d}{2}\big)}\Big)\tilde{g}^2 + \mathcal{O}(\tilde{g}^4), \quad \beta_1^{\tilde{g}} = \mathcal{O}(\tilde{g}^2), \quad \beta_2^{\tilde{g}} = \Big(2\frac{\Gamma\big(\frac{d}{4}\big)^2}{\Gamma\big(\frac{d}{2}\big)}\Big) + \mathcal{O}(\tilde{g}^2). \tag{5.27}$$

It follows that, non-perturbatively, $\beta_{\tilde{g}_1}$ admits two fixed points:

$$\tilde{g}_{1\pm} = \frac{\beta_1^{\tilde{g}} \pm \sqrt{(\beta_1^{\tilde{g}})^2 - \beta_0^{\tilde{g}}\beta_2^{\tilde{g}}}}{\beta_2^{\tilde{g}}} = \pm\sqrt{-\tilde{g}^2} + \mathcal{O}(\tilde{g}^2), \tag{5.28a}$$

$$\beta'_{g_1}(\tilde{g}_{1\pm}) = \pm 2\sqrt{(\beta_1^{\tilde{g}})^2 - \beta_0^{\tilde{g}}\beta_2^{\tilde{g}}} = \pm\sqrt{-\tilde{g}^2}\Big(4\frac{\Gamma\big(\frac{d}{4}\big)^2}{\Gamma\big(\frac{d}{2}\big)}\Big) + \mathcal{O}(\tilde{g}^3). \tag{5.28b}$$

The same holds for $\tilde{g}_2$ substituting $\tilde{g}$ with $\sqrt{q-1}\tilde{g}$, consequently we obtain four lines of fixed points parameterized by the marginal coupling $\tilde{g}$.

Stability. The critical exponents are purely imaginary for $\tilde{g}$ real and not too large, that is the fixed points are limit cycles (see Appendix B) and no trajectory can reach them.

The situation, depicted in Figure 15, is much more interesting for a purely imaginary tetrahedral coupling $\tilde{g} = \pm \mathrm{i}\,|\tilde{g}|$. In this case, the fixed point values of the pillow and double trace couplings are real (for $\tilde{g}$ not too large) and the critical exponents are also real. In particular, $g_{1+} > 0$ and $\beta'_{g_1}(g_{1+}) > 0$, that is, (g_{1+}, g_{2+}) is an infrared attractive fixed point (both the pillow and the double trace couplings are irrelevant).

The tetrahedral invariant does not have any positivity property, but the pillow and double-trace do. It turns out that at the infrared fixed point (g_{1+}, g_{2+}), the real part of the action is bounded from below.

Comparison with $\zeta = 1, d = 4 - \varepsilon$. The case $\tilde{g}$ real is very similar to the Wilson–Fisher-like fixed point discussed in (5.2). In $d = 4 - \varepsilon$ the tetrahedral coupling is not

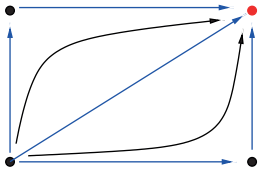

Figure 15. Flows in the (g_1, g_2) plane in the case of imaginary tetrahedral coupling.

marginal (see (5.2)), but has a flow driven by the wave function. The flow has a fixed point for a real value of the tetrahedral coupling.

The key point is that for $\zeta = d/4$ the tetrahedral coupling is genuinely marginal and we are free to chose it purely imaginary. This leads to a stable infrared fixed point.

5.3. The infrared fixed point CFT

The infrared fixed point (g_{1+}, g_{2+}) should be described by a melonic CFT. We will therefore attempt to identify the scaling dimensions and OPE coefficients of this CFT along the lines discussed in Section 2. We consider the four point function

$$\begin{aligned}\frac{1}{N^6}&\langle\phi_A(x_1)\phi_A(x_2)\phi_B(x_3)\phi_B(x_4)\rangle\\ &= \frac{1}{N^3}\langle\phi_A(x_1)\phi_A(x_2)\rangle\frac{1}{N^3}\langle\phi_B(x_3)\phi_B(x_4)\rangle\\ &\quad+\frac{1}{N^6}\langle\phi_A(x_1)\phi_A(x_2)\phi_B(x_3)\phi_B(x_4)\rangle_{12\to 34}.\end{aligned}\tag{5.29}$$

From (4.12), the second term writes in terms of the four point kernel

$$\frac{1}{N^6}\int_{y_1y_2}\Big(\frac{1}{1-K}\Big)_{AA;BB}(x_1,x_2;y_1,y_2)(G_{y_1x_3}G_{y_2x_4}+G_{y_1x_4}G_{y_2x_3}),\tag{5.30}$$

and from (5.8), the four point kernel at leading order in $1/N$ is $K = K_1P_1 + K_2P_2$ with

$$P_1 = 3\Big(\frac{1}{N^2}\delta^p - \frac{1}{N^3}\delta^d\Big),\quad P_2 = \frac{1}{N^3}\delta^d$$

and

$$K_1(x_1,x_2;y_1,y_2) = G_{x_1z_1}G_{x_2z_2}[\lambda^2 G^{q-2}_{z_1z_2} - \lambda_1\delta_{z_1z_2}]\delta_{z_1y_1}\delta_{z_2y_2},\tag{5.31a}$$

$$K_2(x_1,x_2;y_1,y_2) = G_{x_1z_1}G_{x_2z_2}[(q-1)\lambda^2 G^{q-2}_{z_1z_2} - \lambda_2\delta_{z_1z_2}]\delta_{z_1y_1}\delta_{z_2y_2}.\tag{5.31b}$$

Taking into account that $(P_1)_{AA;BB} = 0$ and $(P_2)_{AA,BB} = N^3$, we obtain that only the term proportional to P_2 contributes

$$\frac{1}{N^3} \int\limits_{y_1 y_2} \Big(\frac{1}{1-K_2}\Big)(x_1, x_2; y_1, y_2)(G_{y_1 x_3} G_{y_2 x_4} + G_{y_1 x_4} G_{y_2 x_3}). \tag{5.32}$$

Recalling that the two point function in direct space is

$$G_{xy} = \frac{\Gamma(\Delta_\phi)}{2^{d-2\Delta_\phi} \pi^{d/2} \Gamma\big(\frac{d}{2} - \Delta_\phi\big) Z} \frac{1}{|x-y|^{2\Delta_\phi}}, \tag{5.33}$$

we obtain that the eigenvalues of the kernel $k(\Delta, J)$ (see Section 2) are

$$\begin{aligned} k(\Delta, J) = (q-1)\tilde{g}^2 \;\; & \Gamma(\Delta_\phi)^{q-2} \Gamma\Big(\frac{d}{2} - \Delta_\phi\Big)^2 \\ & \times \frac{\Gamma\big(\Delta_\phi - \frac{d}{2} + \frac{\Delta+J}{2}\big)\Gamma\big(\Delta_\phi - \frac{\Delta-J}{2}\big)}{\Gamma\big(d - \Delta_\phi - \frac{\Delta-J}{2}\big)\Gamma\big(\frac{d}{2} - \Delta_\phi + \frac{\Delta+J}{2}\big)}, \end{aligned} \tag{5.34}$$

with $\Delta_\phi = d/q$. The dimensions of the primary operators as well as the OPE coefficients can be computed starting from this formula. This study has been started in [9] and the dimensions of the spin zero primaries have been analyzed. Surprisingly, for an imaginary (not too large) tetrahedral coupling one finds only real dimensions, while for a real tetrahedral coupling one finds complex dimensions of the form $d/2 + \mathrm{i}\,\alpha$.

An interesting question at this stage is whether this large N CFT is unitary. In order to answer this question, one needs to check whether the leading order OPE coefficients are real. Pursuing this line of inquiry is a very interesting direction of research.

A. The degree

In this appendix we review the degree of edge colored graphs [50, 60] and reproduce the results cited in the main body of this paper. All these results can be found in the literature.

We start by recalling some facts about ribbon graphs. They can be defined formally as combinatorial maps with an additional sign associated to the edges [103] or as graphs embedded in surfaces. Being embedded they have vertices, edges and two-dimensional cells which we call faces. A ribbon graph G can always be projected onto the plane (see Figure 16). The projection of G consists in

- $V(G)$ *ribbon vertices*;
- $E(G)$ *ribbon edges* whose sides we call *strands*. The edges can be straight (parallel strands) or twisted (twisted strands) and can cross. There is at most one twist per edge;
- $F(G)$ *faces*, that is closed strands.

The projection onto the plane is not canonical: by flipping the orientation on some of the vertices, some edges acquire twists and some twists are straightened out.

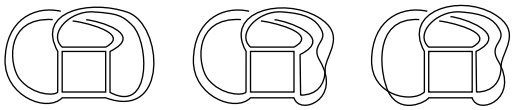

Figure 16. Examples of ribbon graphs with 4 vertices, 6 edges and, from left to right, 2, 2 and 3 faces. From left to right they are embedded into the torus, the Klein bottle and the real projective plane $\mathbb{R}P^2$.

The Euler characteristic of a connected ribbon graph G is

$$V(G) - E(G) + F(G) = 2 - k(G)$$

with $k(G)$ the *non-orientable genus* of G. The genus of a disconnected graph is the sum of the genera of its connected components. A connected ribbon graph with non-orientable genus k is embedded[16] in a surface with non-orientable genus k, that is:

- if $k = 0$ then the graph is *planar* and is embedded in the sphere;
- if k is odd then the graph can only be embedded in a non-orientable surface; ny projection onto the plane will have crossings and twists (see Figure 16, the rightmost case);
- if k is even and non-zero, then either the graph is
  - orientable, that is, embedded in an orientable surface of genus $k/2$. It can be projected onto the plane with only crossing, but no twists (see Figure 16 leftmost case);
  - non-orientable, that is, embedded in a non-orientable surface of non-orientable genus k (see Figure 16, the middle case). Any projection onto the plane will required both crossings and twists.

[16] To be precise, it is embedded in a surface with non-orientable genus at least k and the surface is orientable or not depending on whether the graph is orientable or not.

The edges in a ribbon graph ca be *deleted* (see Figure 17). The deletion of a ribbon edge consists in cutting the edge and joining together the strands at each end of the edge.

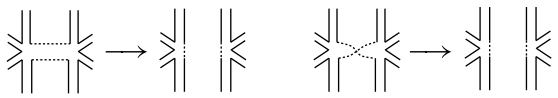

Figure 17. Deletion of an edge.

Let us delete iteratively a maximal set of edges in a connected graph such that at each step the edge we delete separates two different faces. This can not disconnect the graph. The number of edges deleted is $F(G)-1$. The remaining edges connect all the vertices, hence there are at least $V(G)-1$ of them. It follows that the non-orientable genus of a connected ribbon graph is a non-negative integer.

Proposition 1. *Consider a connected ribbon graph G and denote by G' the graph obtained by deleting an edge e. Then,*

- *either G' consists in two connected components G'_1 and G'_2. In this case the genus is distributed between the connected components: $k(G) = k(G'_1) + k(G'_2)$,*
- *or G' is connected an in this case the genus can not increase: $k(G') \leq k(G)$.*

Proof. In the first case, $E(G') = E(G) - 1, V(G') = V(G), F(G') = F(G) + 1$ and the vertices, edges and faces are distributed between the connected components of G'. Then

$$4 - k(G'_1) - k(G'_2) = V(G') - E(G') + F(G') = 2 + 2 - k(G).$$

In the second case, $E(G') = E(G) - 1, V(G') = V(G)$ and $F(G') \geq F(G) - 1$, hence

$$2 - k(G') = V(G') - E(G') + F(G') \geq 2 - k(G).$$ ∎

Figure 18. A triangle with twisted edges in a ribbon graph.

Proposition 2. *A* triangle *in a ribbon graph is a cycle of exactly three edges. If a connected ribbon graph G contains a triangle of twisted edges (see Figure 18), then $k(G) \geq 1$.*

Proof. We delete one by one all the edges incident to the triangle. In the process, the graph G splits into several connected components G_ρ. Let us denote by G_1 the connected component consisting in the triangle. It has 3 (bivalent) vertices, 3 edges and only 1 face, hence $k(G_1) = 1$. Under the deletions, the genus either decreases or is distributed between connected components, thus

$$k(G) \geq \sum_{\rho \geq 1} k(G_\rho) \geq k(G_1) = 1. \qquad \blacksquare$$

A.1. The degree of edge colored graphs

Edge colored graphs have been extensively discussed in detail in the literature [50,55, 60]. We review here some of their properties.

Definition 1. *An* edge $(D+1)$-colored graph $\mathcal{G}$ *is a graph with* $D+1$*-valent vertices and whose edges have a color* $0, 1, \ldots, D$ *such that all the edges incident at a vertex have different colors.*

The faces *with colors* (ij) *of* $\mathcal{G}$ *are the alternating cycles formed by edges with colors* i *and* j*. We denote by* $V(\mathcal{G})$ *the number of vertices and* $F(\mathcal{G})$ *the number of faces of* $\mathcal{G}$*.*

Let us consider a connected edge $(D+1)$-colored graph $\mathcal{G}$. We can project it onto the plane by ordering the edges $0, 1, \ldots, D$ (or any other order) clockwise around the vertices. There are $D!$ cyclic permutations π over the colors $(0, \ldots D)$. We call *jackets* of $\mathcal{G}$ the ribbon graphs indexed by π obtained by keeping all the vertices and edges of $\mathcal{G}$ but only the faces with colors $(\pi^p(0)\pi^{p+1}(0))$. In a ribbon graph representation in which all the edges turn clockwise (following π) around the vertices, all the edges are twisted. Each of these ribbon graphs has a non-orientable genus $k(\pi)$. The *reduced degree* (or simply the *degree*) of $\mathcal{G}$ is the non-negative number

$$\hat{\omega}(\mathcal{G}) = \frac{1}{2(D-1)!} \sum_{\pi} k(\pi) \geq 0. \tag{A.1}$$

The reduced degree of a disconnected graph is the sum of the reduced degrees of its connected components.

Proposition 3. *The total number of faces of a connected edge* $(D+1)$*-colored graph* $\mathcal{G}$ *is*

$$F(\mathcal{G}) = D + \frac{D(D-1)}{4} V(\mathcal{G}) - \hat{\omega}(\mathcal{G}).$$

In particular, the reduced degree is a non-negative half-integer.

Proof. Every face (ij) appears in $2(D-1)!$ cycles: the $(ij\dots)$ cycles and the $(i\dots j)$ cycles. Denoting $F^{(ij)}(\mathcal{G})$ the number of faces with colors (ij) of $\mathcal{G}$, we have

$$V(\mathcal{G}) - \frac{(D+1)}{2}V(\mathcal{G}) + \sum_{p=0}^{D} F^{(\pi^p(0)\pi^{p+1}(0))}(\mathcal{G}) = 2 - k(\pi)$$

$$\Longrightarrow \quad F(\mathcal{G}) = D + \frac{D(D-1)}{4}V(\mathcal{G}) - \frac{1}{2(D-1)!}\sum_{\pi} k(\pi). \qquad \blacksquare$$

The discussion so far applies for $(D+1)$-colored graphs with $D \geq 2$. For $D = 2$, the edge colored graphs are trivalent ribbon graph and the degree is just the genus. The fundamental difference between the $D = 2$ and $D \geq 3$ cases comes from the family of graphs of degree zero. For $D = 2$, they are the (edge 3-colored) planar graphs. For $D \geq 3$ they are melonic graphs.

Definition 2. *The* ring graph *made of an edge of color i closing onto itself and having D faces (with colors (ij) for $j \neq i$) is melonic.*

All melonic graphs are obtained by inserting iteratively two vertices connected by D parallel edges arbitrarily on the edges of lower order melonic graphs. Melonic graphs are always connected.

This definition pertains to vacuum graphs. Cutting any edge in a melonic vacuum graph one obtains a melonic two point graph. Melonic two point graphs are such that their one particle irreducible components factor into D parallel two point functions [61].

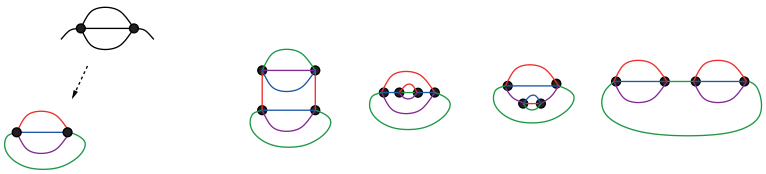

Figure 19. Melonic graphs at first orders

Proposition 4. *For $D \geq 3$, a connected edge $(D+1)$-colored graph $\mathcal{G}$ has reduced degree zero if and only if it is melonic.*

Proof. As the insertion of two vertices connected by D parallel edges brings $\binom{D}{2}$ new faces, it does not change the degree. It follows that melonic graphs have degree zero.

For the converse statement, we proceed by induction on the number of vertices. The faces are cycles with alternating colors hence have even length. We denote by

$F_{2p}(\mathcal{G})$ the number of faces of length $2p$ of $\mathcal{G}$. A vertex contributes $\binom{D+1}{2}$ corners[17] to the faces, thus $\sum_{p\geq 0} 2pF_{2p}(\mathcal{G}) = \frac{(D+1)D}{2}V(\mathcal{G})$. On the other hand,

$$\hat{\omega}(\mathcal{G}) = D + \frac{D(D-1)}{4}V(\mathcal{G}) + \sum_{p\geq 1} F_{2p}(\mathcal{G}),$$

hence,

$$\hat{\omega}(\mathcal{G}) = D + \sum_{p\geq 1} F_{2p}(\mathcal{G})\Big(p\frac{D-1}{D+1} - 1\Big).$$

As $D \geq 3$, the coefficient of $F_{2p}(\mathcal{G})$ is non-negative for all $p \geq 2$. It follows that, if $\hat{\omega}(\mathcal{G}) = 0$ then $F_2(\mathcal{G}) > 0$, that is the graph has at least a face of length exactly 2.

Consider a face of length 2 of $\mathcal{G}$ formed by two edges of colors i and j which join two vertices v and w. If v and w are joined by exactly one edge for all the colors, then the graph is melonic. Let a color c such that two distinct edges of color c are incident to v and w. We call them e_v^c and e_w^c. We consider the jacket $\pi = (icj\ldots)$. This jacket is planar, $k(\pi) = 0$. The two faces on the two sides of e_v^c have colors (i, c) and (j, c) hence are different. Deleting e_v^c, we obtain a connected ribbon graph $\mathcal{J}'_\pi$ having one less face than π, and (using Proposition 1) $k(\mathcal{J}'_\pi) = k(\pi) = 0$. We now delete e_w^c to obtain $\mathcal{J}''_\pi$. This deletion increases the number of faces by 1, $F(\mathcal{J}''_\pi) = F(\mathcal{J}'_\pi) + 1$. If $\mathcal{J}''_\pi$ were connected, we would have $2 - k(\mathcal{J}''_\pi) = 4 \implies k(\mathcal{J}''_\pi) = -2$ which is impossible. Hence, the deletion of e_v^c and e_w^c disconnects the graph $\mathcal{G}$.

Consider the graph obtained from $\mathcal{G}$ by deleting e_v^c and e_w^c and reconnecting the half edges directly in each connected component respecting the colors. It has the same numbers of edges and vertices as $\mathcal{G}$, D more faces (all the faces going through e_v^c and e_w^c are split) and two connected components $\mathcal{G}_1$ and $\mathcal{G}_2$, thus

$$\hat{\omega}(\mathcal{G}_1) + \hat{\omega}(\mathcal{G}_1) = 2D + \frac{D(D-1)}{4}V(\mathcal{G}) - (F + D) = \hat{\omega}(\mathcal{G}) = 0,$$

hence both $\mathcal{G}_1$ and $\mathcal{G}_2$ have degree zero and strictly fewer vertices than $\mathcal{G}$. Iterating, we conclude that $\mathcal{G}$ contains two vertices connected by D parallel edges. ∎

A.2. The SYK degree

Let $D \geq 3$ and denote by $\mathcal{G}^0$ the (possibly disconnected) edge D-colored graph obtained from a connected edge $(D+1)$-colored graph $\mathcal{G}$ by erasing the edges of color 0.[18] Being an edge colored graph, $\mathcal{G}^0$ has a reduced degree $\hat{\omega}(\mathcal{G}^0)$ (defined as in (A.1), but with D shifted to $D-1$).

[17] A corner of a vertex is a couple of half edges $\{i, j\}$.

[18] For $D = 3$, $\mathcal{G}^0$ is a 3-colored graph, hence a trivalent ribbon graph.

Proposition 5. *The SYK degree of a connected edge $(D+1)$-colored graph $\mathcal{G}$*

$$\Omega(\mathcal{G}) = \hat{\omega}(\mathcal{G}) - \hat{\omega}(\mathcal{G}^0), \tag{A.2}$$

is a half-integer which obeys the bounds

$$\frac{1}{D}\hat{\omega}(\mathcal{G}) \leq \Omega(\mathcal{G}) \leq \hat{\omega}(\mathcal{G}). \tag{A.3}$$

The SYK degree is non-negative and it is zero if and only if $\mathcal{G}$ is melonic.

Proof. In order to prove the bounds, we observe that $\mathcal{G}$ has $D!$ jackets and $\mathcal{G}^0$ has $(D-1)!$ jackets. There is a D to one correspondence between the jackets of $\mathcal{G}$ and those of $\mathcal{G}^0$ obtained by erasing the color 0, that is $\pi = (0i \dots j) \to (i \dots j) = \pi^0$. In the associated jacket of $\mathcal{G}$ this corresponds to deleting the edges of color 0. Observe that the graph corresponding to π^0 (which is a jacket of $\mathcal{G}^0$) might be disconnected. The genus can not decrease with the deletions, hence $\sum_\pi k(\pi) \geq D \sum_{\pi^0} k(\pi^0)$. We rewrite the SYK degree as

$$\begin{aligned}\Omega(\mathcal{G}) &= \frac{1}{2(D-1)!}\sum_\pi k(\pi) - \frac{1}{2(D-2)!}\sum_{\pi^0} k(\pi^0) \\ &= \frac{1}{2D(D-2)!}\Big[\sum_\pi k(\pi) - D\sum_{\pi^0} k(\pi^0)\Big] + \frac{1}{2D!}\sum_\pi k(\pi).\end{aligned}$$

The last statements follows from the bounds. ∎

If $\mathcal{G}$ is a melonic graph, then $\mathcal{G}^0$ is a union of melonic graphs. If $\mathcal{G}^0$ happens to have only one connected component, then $\mathcal{G}$ can be uniquely reconstructed from it: in the iterative construction of $\mathcal{G}^0$ one ads an edge of color zero between the pair of vertices inserted at each step.

A.3. The CTKT degree

The graphs of the CTKT model are made of four valent stranded vertices connected by edges with three strands as depicted in Figure 20. The faces are the closed strands and have a color. From left to right in Figure 20 the vertices are the *tetrahedral*, the *pillow* and the *double* trace vertex. There are three kinds of pillow vertices distinguished by the special color which is transmitted from on pair of half edges to the other. We denote by $V_t(\mathcal{G})$, $V_p(\mathcal{G})$, and $V_d(\mathcal{G})$ the numbers of tetrahedral, pillow and double trace vertices and $F(\mathcal{G})$ the number of faces of a graph $\mathcal{G}$.

We aim to define jacket ribbon graphs which will allow us to count the faces. We can not do this naively due to the pillow and double trace vertices. So, we first get

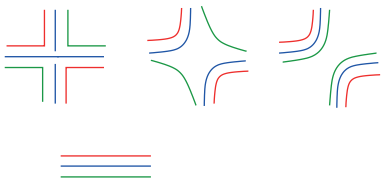

Figure 20. Vertices and edges of the CTKT model

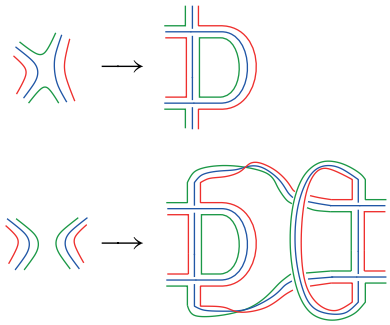

Figure 21. Resolution of the pillow and double trace vertices in terms of the tetrahedral vertex

rid of them. The pillow and double trace vertices can be resolved in terms of minimal configurations of the tetrahedral vertex. This is depicted in Figure 21.

For any graph $\mathcal{G}$, we denote by $\widetilde{\mathcal{G}}$ the graph obtained by replacing all the pillow and double trace vertices by their minimal resolutions in terms of tetrahedral vertices. We call this the *refinement* of $\mathcal{G}$. The refined graph $\widetilde{\mathcal{G}}$ has only tetrahedral vertices and

$$V_t(\widetilde{\mathcal{G}}) = V_t(\mathcal{G}) + 2V_p(\mathcal{G}) + 4V_d(\mathcal{G}), \quad F(\widetilde{\mathcal{G}}) = F(\mathcal{G}) + V_p(\mathcal{G}) + 3V_d(\mathcal{G}).$$

The refined graph $\widetilde{\mathcal{G}}$ admits three jacket ribbon graph $\mathcal{J}^i$ obtained by erasing the faces of the color i. We denote their non-orientable genera by $k(\mathcal{J}^i)$. We define the *CTKT degree* of $\mathcal{G}$ (and of its refinement $\widetilde{\mathcal{G}}$) as

$$\omega(\mathcal{G}) = \frac{1}{2}\sum_i k(\mathcal{J}^i) \geq 0. \tag{A.4}$$

Proposition 6. *The number of faces of a CTKT graph is*

$$F(\mathcal{G}) = 3 + \frac{3}{2}V_t(\mathcal{G}) + 2V_p(\mathcal{G}) + 3V_d(\mathcal{G}) - \omega(\mathcal{G}).$$

Proof. Counting the faces of the refined graph $\widetilde{\mathcal{G}}$ by jacket we find $F(\mathcal{J}^i) = 2 - 2V(\widetilde{\mathcal{G}}) - k(\mathcal{J}^i)$ hence $F(\widetilde{\mathcal{G}}) = 3 + \frac{3}{2}V_t(\widetilde{\mathcal{G}}) - \omega(\mathcal{G})$. Expressing everything in terms

of the numbers of vertices and faces of $\mathcal{G}$ we find

$$F(\mathcal{G}) = 3 + \frac{3}{2}V_t(\widetilde{\mathcal{G}}) - V_p(\mathcal{G}) - 3V_d(\mathcal{G}) - \omega(\mathcal{G})$$
$$= 3 + \frac{3}{2}V_t(\mathcal{G}) + 2V_p(\mathcal{G}) + 3V_d(\mathcal{G}) - \omega(\mathcal{G}). \qquad \blacksquare$$

The CTKT degree is a half-integer. The graphs of degree zero are a slight generalization of the melonic graphs.

Definition 3. *We call a connected CTKT graph $\mathcal{G}$ a* melon-tadpole *graph if its refinement $\widetilde{\mathcal{G}}$ is a melonic graph. Such a graph is obtained by iterated insertions of melons and tadpoles into melons and tadpoles such that all the tadpoles are based at pillow or double trace vertices and all the melons have pairs of tetrahedral vertices. An example is presented in Figure 22*

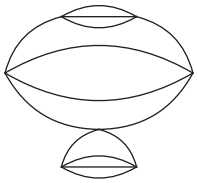

Figure 22. A melon-tadpole graph.

Proposition 7. *A CTKT graph has reduced degree zero if and only if it is a melon-tadpole graph.*

Proof. As $\omega(\mathcal{G}) = \omega(\widetilde{\mathcal{G}})$, this comes to proving that $\widetilde{\mathcal{G}}$ has zero degree if and only if it is melonic. The proof follows the one of Proposition 4, but with some twists. The main difference is that faces can now have odd length.

Assume that the connected graph $\widetilde{\mathcal{G}}$ with only tetrahedral vertices has zero degree. Denoting $F_q(\widetilde{\mathcal{G}})$ the number of faces of length q of $\widetilde{\mathcal{G}}$ and counting corners, we have $\sum_{q\geq 1} qF_q(\widetilde{\mathcal{G}}) = 6V(\widetilde{\mathcal{G}})$. On the other hand, $\omega(\widetilde{\mathcal{G}}) = 3 + \frac{3}{2}V(\widetilde{\mathcal{G}}) - \sum_{q\geq 1} F_q(\widetilde{\mathcal{G}})$, hence we get

$$\omega(\widetilde{\mathcal{G}}) = 3 + \sum_{q\geq 1}\Big(\frac{q}{4} - 1\Big)F_q(\widetilde{\mathcal{G}}).$$

As the faces can now have odd length, $q = 1, 2$, and 3 would have negative coefficients in the above formula. However, we have the following intermediate result.

Lemma 1. *If a connected CTKT graph $\widetilde{\mathcal{G}}$ with only tetrahedral vertices has reduce degree zero, then $F_1(\mathcal{G}) = F_3(\mathcal{G}) = 0$.*

Proof. If $\widetilde{\mathcal{G}}$ has a face of length 1 then it has a tadpole. We build the graph $\widetilde{\mathcal{G}}'$ by replacing the tadpole by an edge. This reduced both the number of edges and faces by 1, hence $\omega(\widetilde{\mathcal{G}}) = \omega(\widetilde{\mathcal{G}}') + 1/2 \geq 1/2$.

Now, assume $\widetilde{\mathcal{G}}$ has a face of length 3 and no tadpoles. Since $\widetilde{\mathcal{G}}$ can not have a tadpole, then the face of length 3 forms a triangle (it can not be a tadpole at the end of a dipole). In the jacket not containing the face of length 3 this leads to a triangle of twisted edges. From Proposition 2, this jacket can not be planar. ∎

Thus, $\widetilde{\mathcal{G}}$ must have a face of length 2 and we conclude by the same induction as in Proposition 4. ∎

B. The renormalization (semi-)group

We briefly review the Wilsonian renormalization group [87] and use this opportunity to introduce some notation.

The one particle irreducible effective action. The generating functional of connected moments of a theory with action $\boldsymbol{S}[\phi]$ is

$$e^{\boldsymbol{W}[J]}7 = \int [d\phi] e^{-\boldsymbol{S}[\phi]+J\cdot\phi},$$
$$\frac{\delta \boldsymbol{W}}{\delta J_x}7 = \langle \phi_x \rangle^J \equiv \boldsymbol{\phi}_x[J], \quad \frac{\delta^2 \boldsymbol{W}}{\delta J_x \delta J_y} = \langle \phi_x \phi_y \rangle_c^{\boldsymbol{J}} = \boldsymbol{G}_{xy}[J],$$

where this time we consider a local source J_x. Going on shell means setting $J = 0$. We denote by $\boldsymbol{J}[\phi]$ the solution of $\boldsymbol{\phi}[J] = \phi$, that is $\boldsymbol{J}[\phi]$ is the source that ensures that the expectation of the field is exactly ϕ. The Legendre transform of $\boldsymbol{W}$ is

$$\boldsymbol{\Gamma}[\phi] = \phi \cdot \boldsymbol{J} - \boldsymbol{W}[\boldsymbol{J}],$$
$$\frac{\delta \boldsymbol{\Gamma}}{\delta \phi_x} = \boldsymbol{J}_x, \quad \frac{\delta^2 \boldsymbol{\Gamma}}{\delta \phi_x \delta \phi_x} = \boldsymbol{G}^{-1}[\phi]_{xy} = (\boldsymbol{G}[J]^{-1}|_{J=\boldsymbol{J}[\phi]})_{xy}.$$

Going on shell means setting $\phi = \phi_0$ solution of the equations of motion $\delta \boldsymbol{\Gamma}/\delta\phi = 0$. From now on, we consider that $\phi_0 = 0$, which can be guaranteed by taking an even action. The effective action can be written as a functional integral

$$e^{-\boldsymbol{\Gamma}[\phi]} = \int [d\psi] e^{-\boldsymbol{S}[\phi+\psi]+\boldsymbol{J}[\phi]\cdot\psi}, \quad \langle \psi \rangle^{\boldsymbol{J}[\phi]} = 0.$$

In this form, $\boldsymbol{J}[\phi]$ is fixed by the requirement that, for the given background ϕ, the expectation of ψ is zero. The above functional integral can be evaluated in a Feynman expansion:

$$e^{-\boldsymbol{\Gamma}[\phi]} = e^{-\boldsymbol{S}[\phi]} \int d\psi e^{-\frac{1}{2}\psi \boldsymbol{S}''[\phi]\psi - \boldsymbol{S}'[\phi]\psi - \sum_{n\geq 3} \frac{1}{n!} \boldsymbol{S}^{(n)}[\phi]\psi^n + \boldsymbol{J}[\phi]\psi}.$$

We have $\mathbf{\Gamma}[\phi] = \boldsymbol{S}[\phi] + \bar{\mathbf{\Gamma}}^{1\mathrm{PI}}[\phi]$, where $-\bar{\mathbf{\Gamma}}^{1\mathrm{PI}}[\phi]$ is the sum over connected vacuum graphs of ψ with propagator $(\boldsymbol{S}''[\phi])^{-1}$, vertices $-\boldsymbol{S}'[\phi]\psi$ and $-\boldsymbol{S}^{(n)}[\phi]\psi^n, n \geq 3$ and a counterterm $\boldsymbol{J}[\phi]\psi$ which ensures that $\langle\psi\rangle^{\boldsymbol{J}[\phi]} = 0$. Observe that the graphs contributing to $\bar{\mathbf{\Gamma}}^{1\mathrm{PI}}[\phi]$ must have edges (i.e., the bare vertices are excluded).

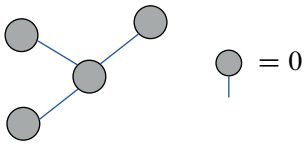

Figure 23. The 1PI decomposition of a graph.

These graphs can always be decomposed along one particle irreducibly edges (that is edges that, when cut, disconnect the graph), as depicted in Figure 23. Every graph is then a tree with vertices the one particle irreducible kernels. Due to the counterterm, the amplitude of any tree having a univalent leaf is zero, hence only the trees with exactly one vertex survive. The tree with one vertex is the sum over all the one particle irreducible graphs. This can be written formally as

$$e^{-\mathbf{\Gamma}[\phi]} = \int_{1\mathrm{PI}} d\psi e^{-\boldsymbol{S}[\phi+\psi]}.$$

There is a slight subtlety here, related to the bare vertices. Let us consider an action consisting in a free part, which is quadratic in the field, and an interaction

$$\boldsymbol{S}[\phi] = \frac{1}{2}\phi \cdot C^{-1} \cdot \phi + \boldsymbol{S}^{\mathrm{int}}[\phi].$$

The interaction $\boldsymbol{S}^{\mathrm{int}}[\phi]$ is conditioned to not have a term proportional to the free part, but it can have other quadratic terms, most notably a mass term. The functional $\bar{\mathbf{\Gamma}}^{1\mathrm{PI}}[\phi]$ contains only graphs with edges hence it does not contain bare vertices. One can include them in the "full 1PI action" $\mathbf{\Gamma}^{1\mathrm{PI}}[\phi] = \boldsymbol{S}^{\mathrm{int}}[\phi] + \bar{\mathbf{\Gamma}}^{1\mathrm{PI}}[\phi]$. The effective action writes

$$\mathbf{\Gamma}[\phi] = \boldsymbol{S}[\phi] + \bar{\mathbf{\Gamma}}^{1\mathrm{PI}}[\phi] = \frac{1}{2}\phi \cdot C^{-1} \cdot \phi + \mathbf{\Gamma}^{1\mathrm{PI}}[\phi].$$

We define the self energy, that is the amputated one particle irreducible 2 point function as

$$\mathbf{\Sigma}[\phi]_{xy} = -\frac{\delta^2 \mathbf{\Gamma}^{1\mathrm{PI}}}{\delta\phi_x \delta\phi_y}, \quad \boldsymbol{G}^{-1}[\phi]_{xy} = (C^{-1})_{xy} - \mathbf{\Sigma}[\phi]_{xy}.$$

The reason to include the bare vertices in the 1PI generating function is that, with this definition, the self energy includes the mass vertex (and also additional quadratic

vertices, if they exist). Observe moreover that

$$e^{-\mathbf{\Gamma}[\phi]} = \int_{1\text{PI}} d\psi e^{-\boldsymbol{S}[\phi+\psi]} = e^{-\frac{1}{2}\phi\cdot C^{-1}\cdot\phi} \int_{1\text{PI}} d\psi e^{-\frac{1}{2}\psi\cdot C^{-1}\cdot\psi+\boldsymbol{S}^{\text{int}}[\phi+\psi]}.$$

Renormalization group flow and fixed points. From now on, we consider the free part of the action to be

$$\frac{1}{2}\int d^d x\phi(x)(-\partial^2)^\zeta\phi(x), \quad C = \frac{1}{(-\partial^2)^\zeta}.$$

with $\zeta \leq 1$. The scaling dimension of the field $\phi(\Omega x) = \Omega^{-\Delta_\phi}\phi(x)$ is dictated by the free part to be $\Delta_\phi = (d-2\zeta)/2$. Observe that the dimension of the field is $[\phi] = [\text{momentum}]^{\Delta_\phi}$.

We introduce an ultraviolet cutoff Λ and an infrared one k and we replace C by C_k^Λ, the covariance with cutoffs.[19] In order to simplify the notation we sometimes suppress the UV cutoff, but one should remember that for now the UV cutoff is present.[20] We parametrize the renormalization group flow by the effective action at scale k:

$$\begin{aligned} e^{-\mathbf{\Gamma}_k[\phi]} =& e^{-\frac{1}{2}\phi\cdot(C_k)^{-1}\cdot\phi} \int_{1\text{PI}} [d\psi] e^{-\frac{1}{2}\psi\cdot(C_k)^{-1}\cdot\psi+\boldsymbol{S}^{\text{int}}[\phi+\psi]}, \\ \mathbf{\Gamma}_k[\phi] =& \frac{1}{n!}\sum_{n\geq 2}\int dx_1\dots dx_n \Gamma_k^{(n)}(x_1,\dots x_n)\phi(x_1)\dots\phi(x_n), \end{aligned} \tag{B.1}$$

where $\Gamma_k^{(n\geq 3)}$ is the n-point amputated 1PI correlation and $\Gamma_k^{(2)}$ is the inverse two point function

$$\Gamma_k^{(2)} = (G_k)^{-1} = (C_k)^{-1} - \Sigma_k,$$

with G_k and Σ_k the two point function and self energy with cutoffs. It follows that the inverse two point function in momentum space takes the form[21]

$$G_k^{-1}(p) = m_k + Z_k p^{2\zeta} + \text{rest},$$

[19] A common choice is to use multiplicative momentum cutoffs $C_k^\Lambda(p) = C(p)\chi_k^\Lambda(p)$, where $\chi_k^\Lambda(p) = \Theta(p^2/\Lambda^2) - \Theta(p^2/k^2)$, and $\Theta(u)$ is some approximated step function cutting off $u \geq 1$.

[20] The cutoffs do not spoil the mass dimension of the field. We have

$$C_k^{-1}(x-y) = \int_p \frac{p^{2\zeta}}{\Theta(p^2/\Lambda^2) - \Theta(p^2/k^2)} e^{-\mathrm{i}\,p(x-y)},$$

hence $C^{-1}_{\Omega^{-1}k}(\Omega(x-y)) = \Omega^{-d-2\zeta}C_k^{-1}(x-y)$ and the quadratic part is invariant under $x \to x' = \Omega x, k \to k' = \Omega^{-1}k$.

[21] The rest term is $p^2 O(p^2/k^2)$ for $\zeta = 1$, while for $\zeta < 1$ it vanishes when lifting the cutoffs.

where $m_k = G_k^{-1}(0)$ is the renormalized mass parameter and Z_k is the wave function renormalization. The free part of the effective action $\phi \cdot G_k^{-1} \cdot \phi$ is dimensionless hence the renormalized field $\sqrt{Z_k}\phi$ has dimension[22] Δ_ϕ. The anomalous dimension of the field is

$$\eta_k = -\frac{1}{2} k \partial_k \ln Z_k, \quad \eta_k \sim O(g^2).$$

It is customary to expand the interaction part of the effective action on a basis of local operators:[23]

$$\mathbf{\Gamma}_k[\phi] = \frac{1}{2}\phi \cdot G_k^{-1} \cdot \phi + \sum_{n,J} k^{d-J-n\Delta_\phi} Z_k^{n/2} g_k^{(n;J)} \int d^d x \partial^J \phi^n(x),$$

where $\partial^J \phi^n(x)$ denotes J derivatives acting on n fields in some order. The explicit Z_k factors in the interaction make $g_k^{(n;J)}$ dimensionless. The β functions are the scale derivatives of the dimensionless couplings:

$$k\partial_k g_k^i = \beta^i(g), \quad \beta^i(g) = (\Delta_i - d) g_k^i + O(g^2),$$

where $i = (n, J)$ and $\Delta_i = J + n\Delta_\phi$ is the classical dimension of $\partial^J \phi^n(x)$. We obtain a fixed point $(\eta_\star, g_\star)$ if

- $\lim_{k\to 0} m_k = 0$, which requires to tune the bare mass in terms of the ultraviolet cutoff Λ;
- $\lim_{k\to 0} \eta_k = \eta_\star$ and $\lim_{k\to 0} \beta^i(g_\star) = 0$.

Taking the ultraviolet cutoff to infinity and tuning the renormalized mass to zero, the only dimensionful parameter we are left with at the fixed point is k. We have $Z_k \overset{k\to 0}{\sim} k^{-2\eta_\star}$ and

$$G_k(x-y) = \frac{k^{2\Delta_\phi}}{Z_k} H(k|x-y|, g_\star) \overset{k\to 0}{\sim} k^{2\Delta_\phi + 2\eta_\star} H(k|x-y|, g_\star),$$

with H some dimensionless function of the dimensionless argument $k|x-y|$ and the fixed point couplings $g_\star$. Taking $k \to 0$, we get the physical two point function

$$G_k(x-y) \overset{k\to 0}{\sim} \frac{c(g_\star)}{|x-y|^{2(\Delta_\phi + \eta_\star)}}.$$

[22] That is, $[\sqrt{Z_k}\phi] = [\text{momentum}]^{\Delta_\phi}$ and under a rescaling of both the positions and the infrared cutoff we have $\sqrt{Z_{\Omega^{-1}k}}\phi(\Omega x) = \Omega^{-\Delta_\phi}\sqrt{Z_k}\phi(x)$.

[23] This is done by Taylor expanding the fields in (B.1) around a position, say x_1:

$$\phi(x_i) = \sum_{q\geq 0} \frac{1}{q!} \sum_{\bar{\mu}=\mu_1\dots\mu_q} (x_i - x_1)^{\bar{\mu}} \partial_{\bar{\mu}} \phi(x_1).$$

In order to explore the neighborhood of the fixed point, let us denote it by ν_a and the eigenvalues of the stability matrix by $\frac{\partial \beta_i}{\partial g_j}(g_\star) = P^{-1}_{ia} \nu_a P_{aj}$. At linear order in the perturbation $g_i = g_{i;\star} + h_i(k)$ around the fixed point, we have

$$h_i(k) = P^{-1}_{ia} \Big(\frac{k}{k_0}\Big)^{\nu_a} P_{aj} h_j(k_0),$$

with k_0 the scale of the initial condition. Thus,

- if $\mathrm{Re}(\nu_a) > 0$, then the eigendirection is irrelevant (the perturbation vanishes for $k \to 0$);
- if $\mathrm{Re}(\nu_a) < 0$, then the eigendirection is relevant (the perturbation grows for $k \to 0$);
- if $\mathrm{Re}(\nu_a) = 0$, then
  - if $\mathrm{Im}(\nu_a) = 0$ the eigendirection is marginal and one gets a line of fixed points;
  - if $\mathrm{Im}(\nu_a) = 0$ the eigendirection is a limit cycle; this case is somewhat pathological because not only no trajectory can ever reach the fixed point, but also the exact value of the coupling at any given scale is strongly dependent on the initial condition.

The scaling dimensions of the operators are $d + \nu_a$. In order to reach the fixed point, one needs to fine tune the relevant couplings (the irrelevant ones flow by themselves to the fixed point values). A fixed point is predictive if it has a small number of relevant directions.

The mass can be separated from the rest of the quadratic terms and treated as an interaction term. It is always classically relevant:

$$k\partial_k m_k = -2\zeta m_k + O(g^2).$$

C. The wave function integral

Let us compute, for $\zeta = d/2 - d/q \leq 1$, the integral

$$I = \int_0^1 dt \int_0^\infty d\alpha \frac{\prod_{i=1}^{q-1} \alpha_i^\zeta}{\big(\sum_{i=1}^{q-1} \prod_{j\neq i} \alpha_j\big)^{d/2+1}} e^{-t \frac{\prod_{i=1}^{q-1} \alpha_i}{\sum_{i=1}^{q-1} \prod_{j\neq i} \alpha_j}}.$$

Changing variables to $\beta = \alpha^{-1}$, rescaling all the βs by t and integrating out t yields

$$I = \frac{1}{\zeta} \int d\beta \frac{\prod_{i=1}^{q-1} \beta_i^{d/2-\zeta-1}}{\big(\sum_{i=1}^{q-1} \beta_i\big)^{d/2+1}} e^{-\frac{1}{\sum_{i=1}^{q-1} \beta_i}}.$$

Introducing $x = \sum_i \beta_i$ and $\beta_i = s_i x$, the integral becomes

$$I = \frac{1}{\zeta} \int_0^\infty dx x^{\zeta-2} e^{-\frac{1}{x}} \int_0^1 \frac{ds_1}{s_1} s_1^{\frac{d}{2}-\zeta} \int_0^{1-s_1} \frac{ds_2}{s_2} s_2^{\frac{d}{2}-\zeta} \dots \int_0^{1-s_1-\dots-s_{q-3}} ds_{q-2} s_{q-2}^{\frac{d}{2}-\zeta-1} (1-s_1-\dots s_{q-2})^{\frac{d}{2}-\zeta-1},$$

and, using

$$\int_0^{1-x} ds s^{a-1} (1-x-s)^{b-1} = (1-x)^{a+b-1} \frac{\Gamma(a)\Gamma(b)}{\Gamma(a+b)},$$

we get

$$I = \frac{\Gamma(1-\zeta)}{\zeta} \frac{\Gamma\left(\frac{d}{2}-\zeta\right)^{q-1}}{\Gamma\left[\left(\frac{d}{2}-\zeta\right)(q-1)\right]} = \frac{\Gamma\left(1-\zeta\right)\Gamma\left(\frac{d}{2}-\zeta\right)^{q-1}}{\zeta\Gamma\left(\frac{d}{2}+\zeta\right)}.$$

References

[1] A. Abdesselam, A complete renormalization group trajectory between two fixed points. *Comm. Math. Phys.* **276** (2007), no. 3, 727–772 Zbl 1194.81168 MR 2350436

[2] J. Ambjørn, B. Durhuus, and T. Jónsson, Three-dimensional simplicial quantum gravity and generalized matrix models. *Modern Phys. Lett. A* **6** (1991), no. 12, 1133–1146 Zbl 1020.83537 MR 1115607

[3] T. Azeyanagi, F. Ferrari, P. Gregori, L. Leduc, and G. Valette, More on the new large D limit of matrix models. *Annals Phys.* **393** (2018), 308–326 Zbl 1390.81287

[4] T. Azeyanagi, F. Ferrari, and F. I. Schaposnik Massolo, Phase diagram of planar matrix quantum mechanics, tensor, and Sachdev–Ye–Kitaev models. *Phys. Rev. Lett.* **120** (2018), no. 6, paper no. 061602 MR 3768708

[5] D. Benedetti, S. Carrozza, R. Gurau, and M. Kolanowski, The $1/N$ expansion of the symmetric traceless and the antisymmetric tensor models in rank three. *Comm. Math. Phys.* **371** (2019), no. 1, 55–97 Zbl 1425.81071 MR 4015340

[6] D. Benedetti, S. Carrozza, R. Gurau, and A. Sfondrini, Tensorial Gross–Neveu models. *J. High Energy Phys.* (2018), no. 1, paper no. 003, Zbl 1384.81077 MR 3764272

[7] D. Benedetti and N. Delporte, Phase diagram and fixed points of tensorial Gross–Neveu models in three dimensions. *J. High Energy Phys.* (2019), no. 1, paper no. 218

[8] D. Benedetti and R. Gurau, 2PI effective action for the SYK model and tensor field theories. *J. High Energy Phys.* (2018), paper no. 5 Zbl 1391.81116 MR 3815031

[9] D. Benedetti, R. Gurau, and S. Harribey, Line of fixed points in a bosonic tensor model. *J. High Energy Phys.* (2019), no. 6, paper no. 053 Zbl 1416.81113 MR 3979830

[10] J. Ben Geloun and V. Rivasseau, A renormalizable 4-dimensional tensor field theory. *Comm. Math. Phys.* **318** (2013), no. 1, 69–109 Zbl 1261.83016 MR 3017064

[11] J. Berges, Introduction to nonequilibrium quantum field theory. *AIP Conf. Proc.* **739** (2005), 3–62

[12] T. H. Berlin and M. Kac, The spherical model of a ferromagnet. *Phys. Rev. (2)* **86** (1952), 821–835 Zbl 0047.45703 MR 49829

[13] V. Bonzom, R. Gurau, A. Riello and V. Rivasseau, Critical behavior of colored tensor models in the large N limit. *Nucl. Phys. B* **853** (2011) 174–195 Zbl 1229.81222 MR 2831765

[14] V. Bonzom, R. Gurau, J. P. Ryan, and A. Tanasa, The double scaling limit of random tensor models. *J. High Energy Phys.* (2014), no. 9, paper no. 051 Zbl 1333.60014 MR 3268519

[15] P. Breitenlohner and D. Z. Freedman, Stability in gauged extended supergravity. *Ann. Physics* **144** (1982), no. 2, 249–281 Zbl 0606.53044 MR 684223

[16] E. Brézin, C. Itzykson, G. Parisi, and J. B. Zuber, Planar diagrams. *Comm. Math. Phys.* **59** (1978), no. 1, 35–51 Zbl 0997.81548 MR 471676

[17] É. Brézin and V. A. Kazakov, Exactly solvable field theories of closed strings. *Phys. Lett. B* **236** (1990), no. 2, 144–150 MR 1040213

[18] D. C. Brydges, P. K. Mitter and B. Scoppola, Critical $(\Phi^4)_{3,\varepsilon}$. *Commun. Math. Phys.* **240** (2003), no. 1–2, 281–327 Zbl 1053.81065 MR 2004988

[19] K. Bulycheva, I. R. Klebanov, A. Milekhin, and G. Tarnopolsky, Spectra of operators in large N tensor models. *Phys. Rev. D* **97** (2018), no. 2, paper no. 026016 MR 3877831

[20] S. Carrozza, Large N limit of irreducible tensor models: O(N) rank-3 tensors with mixed permutation symmetry. *J. High Energy Phys.* (2018), no. 6, paper no. 039 Zbl 1395.81155 MR 3850828

[21] S. Carrozza and V. Pozsgay, SYK-like tensor quantum mechanics with Sp(N) symmetry. *Nuclear Phys. B* **941** (2019), 28–52 Zbl 1415.81131 MR 3916553

[22] S. Carrozza and A. Tanasa, $O(N)$ random tensor models. *Lett. Math. Phys.* **106** (2016), no. 11, 1531–1559 MR 3555413

[23] S. Choudhury, A. Dey, I. Halder, L. Janagal, S. Minwalla, and R. R. Poojary, Notes on melonic O$(N)^{q-1}$ tensor models. *J. High Energy Phys.* (2018), no. 6, paper no. 094 Zbl 1395.83106 MR 3831773

[24] J. M. Cornwall, R. Jackiw and E. Tomboulis, Effective action for composite operators. *Phys. Rev. D* **10** (1974)o no. 2428–2445 Zbl 1110.81324

[25] M. S. Costa, J. Penedones, D. Poland, and S. Rychkov, Spinning conformal blocks. *J. High Energy Phys.* (2011), no. 11, paper no. 154 Zbl 1306.81148

[26] S. Dartois, R. Gurau, and V. Rivasseau, Double scaling in tensor models with a quartic interaction. *J. High Energy Phys.* (2013), no. 9, paper no. 088 Zbl 1342.83079 MR 3102990

[27] P. Di Francesco, P. Ginsparg, and J. Zinn-Justin, 2D gravity and random matrices. *Phys. Rep.* **254** (1995), no. 1–2, 1–133 MR 1320471

[28] P. Di Francesco, P. Mathieu, and D. Sénéchal, *Conformal field theory*. Grad. Texts Contemp. Phys., Springer, New York, 1997 Zbl 0869.53052 MR 1424041

[29] F. A. Dolan and H. Osborn, Conformal four point functions and the operator product expansion. *Nuclear Phys. B* **599** (2001), no. 1-2, 459–496 Zbl 1097.81734 MR 1826467

[30] M. R. Douglas and S. H. Shenker, Strings in less than one dimension. *Nuclear Phys. B* **335** (1990), no. 3, 635–654 MR 1059822

[31] F. Ferrari, The large D limit of planar diagrams. *Ann. Inst. Henri Poincaré D* **6** (2019), no. 3, 427–448 Zbl 1431.83092 MR 4002672

[32] F. Ferrari, V. Rivasseau, and G. Valette, A new large N expansion for general matrix-tensor models. *Comm. Math. Phys.* **370** (2019), no. 2, 403–448 Zbl 07100582 MR 3994575

[33] F. Ferrari and F. I. Schaposnik Massolo, Phases of melonic quantum mechanics. *Phys. Rev. D* **100** (2019), no. 2, paper no. 026007 MR 4017334

[34] E. S. Fradkin and M. A. Vasiliev, Cubic interaction in extended theories of massless higher-spin fields. *Nuclear Phys. B* **291** (1987), no. 1, 141–171 MR 895978

[35] E. S. Fradkin and M. A. Vasilev, On the gravitational interaction of massless higher-spin fields. *Phys. Lett. B* **189** (1987), no. 1–2, 89–95 Zbl 0967.81517 MR 890906

[36] É. Fusy, L. Lionni, and A. Tanasa, Combinatorial study of graphs arising from the Sachdev–Ye–Kitaev model. *European J. Combin.* **86** (2020), paper no. 103066 Zbl 1437.05103 MR 4053712

[37] M. Gell-Mann, *Murray Gell-Mann: selected papers*. Edited by H. Fritzsch, World Sci. Ser. 20th Century Phys. 40, World Scientific Publishing Co., Hackensack, NJ, 2010 Zbl 1188.01026 MR 2766463

[38] S. Giombi, I. R. Klebanov, F. Popov, S. Prakash, and G. Tarnopolsky, Prismatic large N models for bosonic tensors. *Phys. Rev. D* **98** (2018), no. 10, paper no. 105005 MR 3954724

[39] S. Giombi, I. R. Klebanov, and G. Tarnopolsky, Bosonic tensor models at large N and small ε. *Phys. Rev. D* **96** (2017), no. 10, paper no. 106014 MR 3867822

[40] S. L. Glashow, Partial symmetries of weak interactions. *Nucl. Phys.* **22** (1961), 579–588

[41] J. Glimm and A. Jaffe, *Quantum physics*. Second edn., Springer, New York, 1987 Zbl 0461.46051 MR 887102

[42] D. J. Gross and A. A. Migdal, Nonperturbative two-dimensional quantum gravity. *Phys. Rev. Lett.* **64** (1990), no. 2, 127–130 Zbl 1050.81610 MR 1031944

[43] D. J. Gross and V. Rosenhaus, A generalization of Sachdev–Ye–Kitaev. *J. High Energy Phys.* (2017), paper no. 093 Zbl 1377.81172 MR 3637521

[44] D. J. Gross and V. Rosenhaus, A line of CFTs: from generalized free fields to SYK. *J. High Energy Phys.* (2017), no. 7, paper no. 086 Zbl 1380.81323 MR 3686712

[45] D. J. Gross and V. Rosenhaus, All point correlation functions in SYK. *J. High Energy Phys.* (2017), no. 12, paper no. 148 Zbl 1383.81218 MR 3756642

[46] D. J. Gross and V. Rosenhaus, The bulk dual of SYK: cubic couplings. *J. High Energy Phys.* (2017), paper no. 092 Zbl 1380.81322 MR 3662839

[47] S. S. Gubser and I. R. Klebanov, A Universal result on central charges in the presence of double trace deformation. *Nucl. Phys. B* **656** (2003), no. 1–2, 23–36 Zbl 1011.81067

[48] S. S. Gubser, I. R. Klebanov, and A. M. Polyakov, Gauge theory correlators from non-critical string theory. *Phys. Lett. B* **428** (1998), no. 1–2, 105–114 Zbl 1355.81126

[49] R. Guida and J. Zinn-Justin, Critical exponents of the N-vector model. *J. Phys. A* **31** (1998), no. 40, 8103–8121 Zbl 0978.82037 MR 1651491

[50] R. Gurau, Colored group field theory. *Comm. Math. Phys.* **304** (2011), no. 1, 69–93 Zbl 1214.81170 MR 2793930

[51] R. Gurau, The $1/N$ expansion of colored tensor models. *Ann. Henri Poincaré* **12** (2011), no. 5, 829–847 Zbl 1218.81088 MR 2802384

[52] R. Gurau, The complete $1/N$ expansion of colored tensor models in arbitrary dimension. *Ann. Henri Poincaré* **13** (2012), no. 3, 399–423 Zbl 1245.81118 MR 2909101

[53] R. Gurau, The $1/N$ expansion of tensor models beyond perturbation theory. *Comm. Math. Phys.* **330** (2014), no. 3, 973–1019 Zbl 1297.81126 MR 3227505

[54] R. Gurau, Quenched equals annealed at leading order in the colored SYK model. Europhys. Lett. **119** (2017), no. 3, paper no. 30003

[55] R. Gurau, *Random tensors*. Oxford University Press, Oxford, 2017 Zbl 1371.81007 MR 3616422

[56] R. Gurau, The complete $1/N$ expansion of a SYK-like tensor model. *Nuclear Phys. B* **916** (2017), 386–401 Zbl 1356.81180 MR 3611412

[57] R. Gurau, The $1/N$ expansion of tensor models with two symmetric tensors. *Comm. Math. Phys.* **360** (2018), no. 3, 985–1007 Zbl 1393.81026 MR 3803815

[58] R. Gurau and T. Krajewski, Analyticity results for the cumulants in a random matrix model. *Ann. Inst. Henri Poincaré D* **2** (2015), no. 2, 169–228 Zbl 1353.60009 MR 3354330

[59] R. Gurau and V. Rivasseau, The $1/N$ expansion of colored tensor models in arbitrary dimension. *Europhys. Lett* **95** (2011), paper no. 5000

[60] R. Gurau and J. P. Ryan, Colored tensor models – a review. *SIGMA Symmetry Integrability Geom. Methods Appl.* **8** (2012), article no. 020 Zbl 1242.05094 MR 2942819

[61] R. Gurau and G. Schaeffer, Regular colored graphs of positive degree. *Ann. Inst. Henri Poincaré D* **3** (2016), no. 3, 257–320 Zbl 1352.05090 MR 3549799

[62] R. Gurau, A. Tanasa, and D. R. Youmans, The double scaling limit of the multi-orientable tensor model. *Europhys. Lett.* **111** (2015), no. 2, paper no. 21002

[63] E. Ising, Contribution to the theory of ferromagnetism. *Z. Phys.* **31** (1925) 253–258 Zbl 1439.82056

[64] G. Jona-Lasinio, Relativistic field theories with symmetry breaking solutions. *Nuovo Cimento* **34** (1964), 1790–1795

[65] J. Kim, I. R. Klebanov, G. Tarnopolsky and W. Zhao, Symmetry breaking in coupled SYK or tensor Models. 2019, arXiv:1902.02287

[66] A. Kitaev, A simple model of quantum holography. Entanglement in Strongly-Correlated Quantum Matter, KITP, 2015
Part I. https://online.kitp.ucsb.edu/online/entangled15/kitaev/
Part II. https://online.kitp.ucsb.edu/online/entangled15/kitaev2/

[67] I. R. Klebanov, A. Milekhin, F. Popov, and G. Tarnopolsky, Spectra of eigenstates in fermionic tensor quantum mechanics. *Phys. Rev. D* **97** (2018), no. 10, paper no. 106023 MR 3886101

[68] I. R. Klebanov, P. N. Pallegar, and F. K. Popov, Majorana fermion quantum mechanics for higher rank tensors. *Phys. Rev. D* **100** (2019), no. 8, paper no. 086003 MR 4032019

[69] I. R. Klebanov and A. M. Polyakov, AdS dual of the critical O(N) vector model. *Phys. Lett. B* **550** (2002), no. 3-4, 213–219 Zbl 1001.81057 MR 1948547

[70] I. R. Klebanov, F. Popov, and G. Tarnopolsky, TASI lectures on large N tensor models. In *Theoretical Advanced Study Institute Summer School 2017 "Physics at the Fundamental Frontier" (TASI2017),* Proceedings of Science, 2018, paper no. 004 https://pos.sissa.it/305/004/pdf

[71] I. R. Klebanov and G. Tarnopolsky, On large N limit of symmetric traceless tensor models. *J. High Energy Phys.* (2017), no. 10, paper no. 037 Zbl 1383.81239 MR 3731176

[72] I. R. Klebanov and G. Tarnopolsky, Uncolored random tensors, melon diagrams, and the SYK Models. *Phys. Rev. D* **95** (2017), no. 4, paper no. 046004

[73] T. Krajewski, V. Rivasseau, and V. Sazonov, Constructive matrix theory for higher-order interaction. *Ann. Henri Poincaré* **20** (2019), no. 12, 3997–4032 Zbl 1426.81048 MR 4025785

[74] T. Krajewski, V. Rivasseau, A. Tanasă, and Z. Wang, Topological graph polynomials and quantum field theory. I. Heat kernel theories. *J. Noncommut. Geom.* **4** (2010), no. 1, 29–82 Zbl 1186.81095 MR 2575389

[75] C. Krishnan and K. V. Pavan Kumar, Towards a finite-N hologram. *J. High Energy Phys.* (2017), paper no. 099 Zbl 1383.81240 MR 3731114

[76] C. Krishnan and K. V. Pavan Kumar, Exact solution of a strongly coupled gauge theory in $0 + 1$ dimensions. *Phys. Rev. Lett.* **120** (2018), no. 20, paper no. 201603

[77] C. Krishnan, K. V. Pavan Kumar, and D. Rosa, Contrasting SYK-like models. *J. High Energy Phys.* (2018), no. 1, paper no. 64 Zbl 1384.83061

[78] C. Krishnan, S. Sanyal, and P. N. B. Subramanian, Quantum chaos and holographic tensor models. *J. High Energy Phys.* (2017), no. 3, paper no. 056 Zbl 1377.83049 MR 3657641

[79] J. Liu, E. Perlmutter, V. Rosenhaus, and D. Simmons-Duffin, d-dimensional SYK, AdS loops, and $6j$ symbols. *J. High Energy Phys.* (2019), no. 3, paper no. 052 Zbl 1414.81211 MR 3951214

[80] J. Maldacena and D. Stanford, Remarks on the Sachdev–Ye–Kitaev model. *Phys. Rev. D* **94** (2016), no. 10, paper no. 106002 MR 3751002

[81] W. Metzner, M. Salmhofer, C. Honerkamp, V. Meden, and K. Schonhammer, Functional renormalization group approach to correlated fermion systems. *Rev. Mod. Phys.* **84** (2012), paper no. 299

[82] M. Moshe and J. Zinn-Justin, Quantum field theory in the large N limit: a review. *Phys. Rep.* **385** (2003), no. 3-6, 69–228 Zbl 1031.81065 MR 2010168

[83] K. Pakrouski, I. R. Klebanov, F. Popov, and G. Tarnopolsky, Spectrum of Majorana quantum mechanics with $O(4)^3$ symmetry. *Phys. Rev. Lett.* (2019), no. 1, paper no. 011601

[84] D. Pappadopulo, S. Rychkov, J. Espin and R. Rattazzi, OPE convergence in conformal field theory. *Phys. Rev. D* **86** (2012), paper no. 105043

[85] R. Pascalie, C. I. Pérez-Sánchez, A. Tanasa, and R. Wulkenhaar, On the large N limit of Schwinger–Dyson equations of a rank-3 tensor field theory. *J. Math. Phys.* **60** (2019), no. 7, article no. 073502 Zbl 1420.81024 MR 3976423

[86] C. Peng, M. Spradlin, and A. Volovich, A supersymmetric SYK-like tensor model. *J. High Energy Phys.* (2017), no. 5, article no. 062 Zbl 1380.81355 MR 3662869

[87] M. E. Peskin, *An introduction to quantum field theory*. CRC Press, Boca Raton, 2018

[88] J. Polchinski, Renormalization and effective Lagrangians. *Nucl. Phys. B* **231** (1984), 269–295

[89] J. Polchinski and V. Rosenhaus, The spectrum in the Sachdev–Ye–Kitaev model. *J. High Energy Phys.* (2016), no. 4, paper no. 001 Zbl 1388.81067 MR 3512315

[90] F. K. Popov, Supersymmetric tensor model at large N and small ε. *Phys. Rev. D* **101** (2020), no. 2, article no. 026020, 15 MR 4069170

[91] S. Prakash and R. Sinha, A complex fermionic tensor model in d dimensions. *J. High Energy Phys.* (2018), no. 2, article no. 086 Zbl 1387.81330 MR 3785166

[92] V. Rivasseau, *From perturbative to constructive renormalization*. Princeton Ser. Phys., Princeton University Press, Princeton, NJ, 1991 MR 1174294

[93] V. Rivasseau and F. Vignes-Tourneret, Constructive tensor field theory: the T_4^4 model. *Comm. Math. Phys.* **366** (2019), no. 2, 567–646. Zbl 1417.81148 MR 3922533

[94] S. Sachdev and J. Ye, Gapless spin fluid ground state in a random, quantum Heisenberg magnet. *Phys. Rev. Lett.* **70** (1993), paper no. 3339

[95] A. Salam, Weak and electromagnetic interactions. 8th Nobel Symposium. *Conf. Proc.* **680519** (1968) 367–377; reprinted in *Selected Papers of Abdus Salam,* pp. 244-254, World Scientific Series in 20th Century Physics 5, World Scientific, Singapore etc., 1994

[96] D. O. Samary, C. I. Pérez-Sánchez, F. Vignes-Tourneret, and R. Wulkenhaar, Correlation functions of a just renormalizable tensorial group field theory: the melonic approximation. *Classical Quantum Gravity* **32** (2015), no. 17, paper no. 175012 Zbl 1327.83122 MR 3382874

[97] N. Sasakura, Tensor model for gravity and orientability of manifold. *Modern Phys. Lett. A* **6** (1991), no. 28, 2613–2623 Zbl 1020.83542 MR 1125467

[98] S. El-Showk, M. F. Paulos, D. Poland, S. Rychkov, D. Simmons-Duffin, and A. Vichi, Solving the 3d Ising model with the conformal bootstrap. *Phys. Rev. D* **86** (2012), paper no. 025022

[99] D. Simmons-Duffin, D. Stanford, and E. Witten, A spacetime derivation of the Lorentzian OPE inversion formula. *J. High Energy Phys.* (2018), no. 7, paper no. 085 Zbl 1395.81246 MR 3861968

[100] H. E. Stanley, Spherical model as the limit of infinite spin dimensionality. *Phys. Rev.* **176** (1968), 718–722

[101] G. 't Hooft, Planar diagram theory for strong interactions. *Nucl. Phys. B* **72** (1974), no. 3, 461-473

[102] M. A. Vasiliev, Higher spin gauge theories: star-product and AdS space. In *The many faces of the superworld*, pp. 533–610, World Sci. Publ., River Edge, NJ, 2000 Zbl 0990.81084 MR 1885992

[103] F. Vignes-Tourneret, The multivariate signed Bollobás–Riordan polynomial. *Discrete Math.* **309** (2009), no. 20, 5968–5981 Zbl 1228.05183 MR 2552629

[104] S. Weinberg, A model of leptons. *Phys. Rev. Lett.* **19** (1967), 1264–1266

[105] K. G. Wilson and M. E. Fisher, Critical exponents in 3.99 dimensions. *Phys. Rev. Lett.* **28** (1972), 240–243

[106] K. G. Wilson and J. B. Kogut, The renormalization group and the epsilon expansion. *Phys. Rept.* **12** (1974), 75–199

[107] E. Witten, Anti de Sitter space and holography. *Adv. Theor. Math. Phys.* **2** (1998), no. 2, 253–291 Zbl 0914.53048 MR 1633012

[108] E. Witten, An SYK-like model without disorder. *J. Phys. A* **52** (2019), no. 47, paper no. 474002 MR 4028950

[109] J. Zinn-Justin, *Quantum field theory and critical phenomena*. Third edn., Int. Ser. Monogr. Phys. 85, The Clarendon Press, Oxford University Press, New York, 1996 Zbl 0865.00014

Communicated by Adrian Tanasă

Received 16 July 2019.

Razvan Gurau
CPHT, CNRS, Ecole Polytechnique, Institut Polytechnique de Paris, Route de Saclay,
91128 Palaiseau, France; and Perimeter Institute for Theoretical Physics,
31 Caroline Street North, Waterloo, Ontario N2L 2Y5, Canada; rgurau@cpht.polytechnique.fr